Optical and photoreceptor immaturities limit the spatial and chromatic vision of human neonates

Martin S. Banks

School of Optometry, University of California, Berkeley, Berkeley, California 94720

Patrick J. Bennett

Department of Psychology, University of California, Berkeley, Berkeley, California 94720

Received May 25, 1988; accepted August 18, 1988

We examine the contributions of preneural mechanisms, i.e., the optics of the eye and the aperture, spacing, and efficiency of foveal cones, to poor spatial and chromatic vision in human neonates. We do so by comparing the performances of ideal observers incorporating the characteristics of the optics and the foveal cones of adults and neonates. Our analyses show that many, but not all, of the differences between neonatal and adult contrast sensitivities and grating acuities can be explained by age-related changes in these factors. The analyses also predict differing growth curves for vernier and grating acuities. Finally, we demonstrate that preneural mechanisms constrain chromatic discrimination in human neonates and that discrimination failures may reflect poor visual efficiency rather than immature chromatic mechanisms *per se*.

1. INTRODUCTION

Human neonates see poorly. Contrast sensitivity, grating acuity, and vernier acuity in the first month of life are all at least an order of magnitude worse than in adulthood. Chromatic discrimination is much reduced, too. One would think that such striking functional deficits would have obvious anatomical and physiological causes, yet the specific causes are still debated. In regard to spatial vision, several investigators have proposed that photoreceptor immaturities are the primary constraint,[1,2] but others have emphasized immaturities among retinal neurons and the central nervous system.[3–5] In regard to chromatic vision, early deficits have been attributed to immaturities among chromatic mechanisms.[6] Here we examine the factors that limit spatial vision and chromatic vision in human neonates. Specifically, we evaluate the extent to which early visual deficits can be explained by information losses at the front end of the visual system. We conclude that many, but not all, of the spatial and chromatic deficits can be explained by optical and photoreceptor immaturities. Calculations of these front-end information losses allow us to estimate the magnitude and the character of postreceptoral losses. Such estimates should be useful in the construction of models of the development of postreceptoral mechanisms.

Our approach relies on ideal-observer theory. By definition, the performance of an ideal observer is optimal, given the physical and physiological constraints that are built in. Ideal observers are useful tools in vision research because their performance provides a rigorous measure of the information available at chosen processing stages.[7–11] For instance, the performance of an ideal observer with the optical and photoreceptor properties of an adult eye reveals the information available at the receptors for discriminating among various spatial and chromatic stimuli. Similarly, comparing the performance of two ideal observers with different optics and receptors reveals how differences in those properties affect discrimination information. In this sense, ideal-observer analyses permit an atheoretic assessment of constraints imposed by various stages of visual processing.

Here we derive an ideal observer with the optical and photoreceptor characteristics of the human newborn fovea. These characteristics now are understood well enough to minimize the number of necessary assumptions. The performance of this ideal observer is then computed for various spatial and chromatic tasks. It is the best possible for a visual system with the front end of the newborn system. Comparisons of the performances of newborn and adult ideal observers reveal the information lost by optical and photoreceptor immaturities across the life span. We show that many, but not all, of the deficits that human neonates exhibit in contrast sensitivity, grating acuity, vernier acuity, and chromatic discrimination can be attributed to information losses in the optics and the photoreceptors.

2. THE NEONATAL IDEAL OBSERVER

In this section we describe and justify the parameters built into the neonatal ideal observer. The existing quantitative data on photoreceptor development have rather large gaps in the age distribution, and so we limit our discussion mostly to newborns and adults.

A. Optics

Four optical properties are important to the derivation of an ideal observer for spatial and chromatic visual tasks: posterior nodal distance, pupil size, ocular media transmittance, and the optical transfer function. As shown in Table 1, we used posterior nodal distances of 11.7 and 16.7 mm for newborns and adults, respectively.[12–17] Image magnification is proportional to posterior nodal distance, so the adult eye is

0740-3232/88/122059-21$02.00

Table 1. Ideal-Observer Parameters

Factor	Source	Neonate Foveal Slope	Central Fovea		
			Neonate	15-Month-Old Infant	Adult
Pupil diameter	Salapatek and Banks[14]	2.2 mm	2.2 mm	2.7 mm	3.3 mm
Axial length	Larsen,[13] Stenstrom[15]	16.6 mm	16.6 mm	20.4 mm	24.0 mm
Posterior nodal distance	Axial length ratios	11.7 mm	11.7 mm	14.4 mm	16.7 mm
Receptor aperture	Yuodelis and Hendrickson,[16] Miller and Bernard[17]	0.35 arcmin	0.35 arcmin	0.67 arcmin	0.48 arcmin
Receptor spacing	Youdelis and Hendrickson[16]	1.66 arcmin	2.30 arcmin	1.27 arcmin	0.58 arcmin

suited better than the shorter newborn eye for detail vision. Also, as shown in Table 1, we assumed pupil diameters of 2.2 and 3.3 mm for newborns and adults, respectively. Retinal illuminance is proportional to the eye's numerical aperture (the pupil diameter divided by the posterior focal length). The numerical apertures of newborn and adult eyes are similar because the age-related increases in pupil diameter and posterior nodal distance are similar. Consequently, the retinal illuminance associated with a given target luminance is probably similar in newborns and adults.[14,18]

Two elements affecting ocular media transmittance are known to change with age: the crystalline lens and macular pigments. In both cases, transmittance is higher in the young eye,[19,20] but the differences between newborn and adult eyes are small at all but short wavelengths. We assumed optical densities at 400 nm of 1.00 and 1.35 for the newborn and adult lenticular pigments and densities at 450 nm of 0.0 and 0.50 for newborn and adult macular pigments.

No measurements have been made (to our knowledge) of the OTF of the human neonatal eye, but it is likely that the optical quality of the newborn eye greatly exceeds the resolution performance of the system as a whole.[21-23] We assumed therefore that the OTF of the newborn eye is similar to that of the adult eye. Specifically, we used the transfer function of Campbell and Gubisch[24] for a 3-mm adult pupil and white light.

B. Photoreceptors

Several investigators have reported that the central retina is quite immature at birth.[16,20,25] The fovea develops rapidly in the first year, but subtle morphological changes continue until at least 4 years of age.[16] Figure 1 displays the human

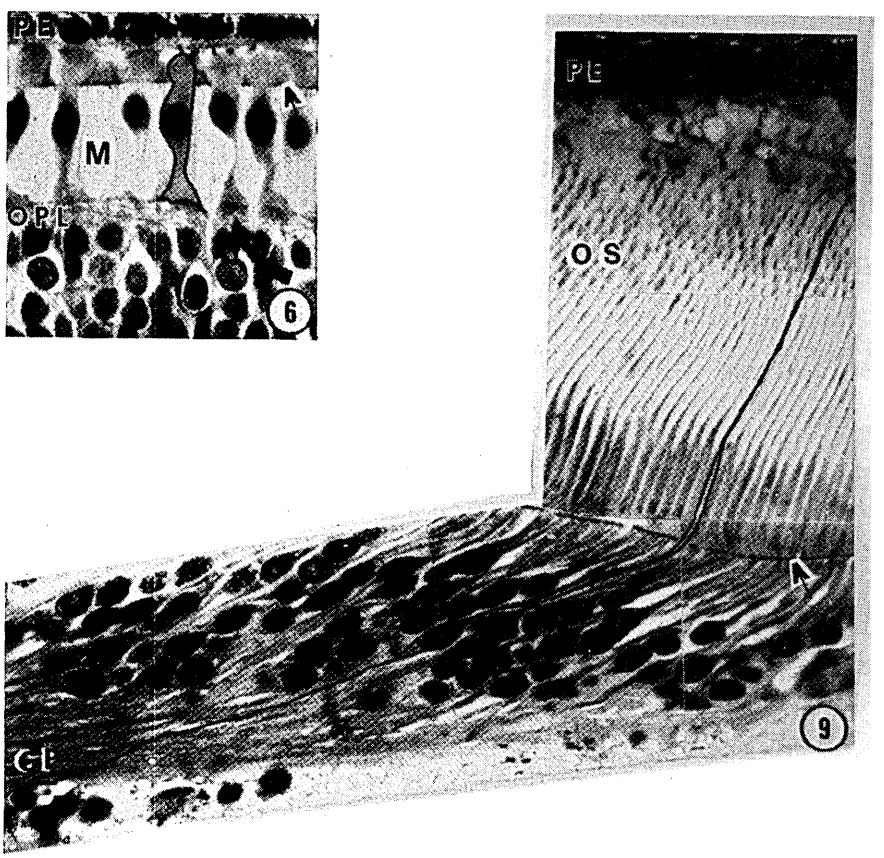

Fig. 1. Development of human foveal cones illustrated by light micrographs. A single cone is outlined in each figure; magnification in all figures is constant. Ages: six, 5 days postpartum; nine, 72 years. PE, Pigment epithelium; OPL, outer plexiform layer; M, Muller glial cell processes; CP, cone synaptic pedicles; OS, outer segments. (Reprinted from Ref. 16.)

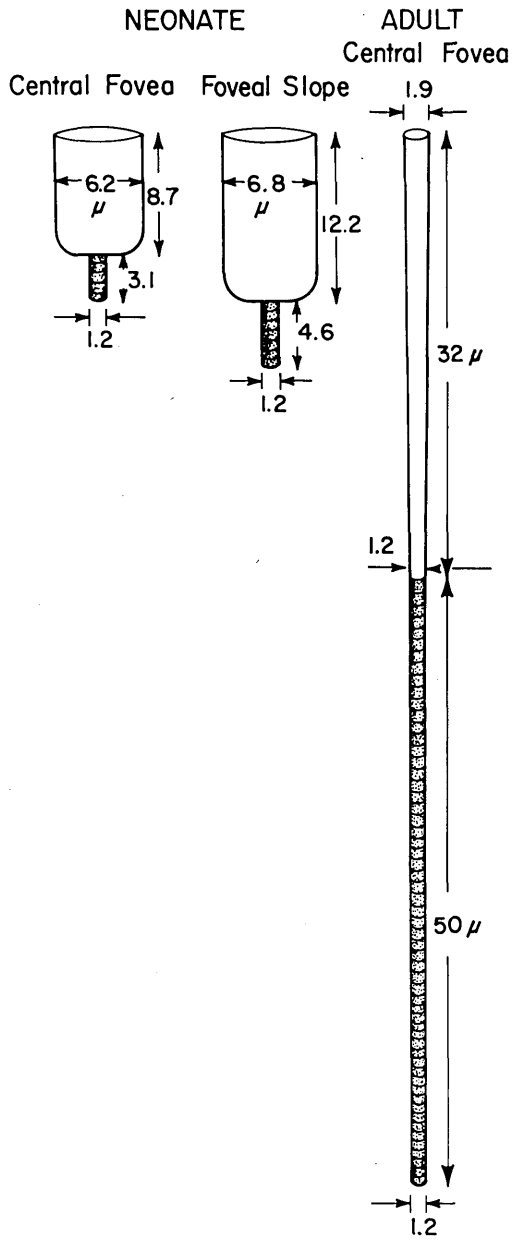

Fig. 2. Dimensions (in micrometers) and shapes used to model neonate and adult foveal cones. On the left is the model cone used for the central 250 μm of the neonate's fovea. The inner segment is not tapered, in accord with the observations of Yuodelis and Hendrickson.[16] In the middle is the model cone used for the foveal slope of the neonate. Again, the inner segment is untapered. On the right is the cone used to represent mature central foveal cones.

foveola at birth and in adulthood. The diameter of the foveola (defined by the rod-free zone) decreases from roughly 5.4 deg at birth to 2.3 deg at maturity.[26] An individual cone is outlined for clarity in each panel. The outer segments of the cones are labeled OS. The inner segments are just below the outer segments. These beautiful micrographs illustrate the striking morphological differences between neonatal and adult cones. Neonatal inner segments are much broader and shorter and, in contrast to their mature counterparts, are not tapered from the external limiting membrane to the interface with the outer segment. The outer segments are distinctly immature, too, being much shorter than their adult counterparts.

We calculated the ability of the newborn's cones to capture light in the inner segment, to funnel it to the outer segment, and to produce an isomerization. We used geometric optics and a ray-trace program to estimate the effective collecting areas of newborn cones.[27] The cone shapes used to make these calculations are based on the measurements of Yuodelis and Hendrickson[16] and are shown in Fig. 2. Separate analyses were conducted for cones in the central fovea and on the foveal slope (approximately 3 deg from the foveal center) because they differ morphologically. Refractive indices were set to values for a mature eye. We found that the waveguide of the inner segment cannot work properly. The reason is as follows. The inner segment is short and much broader than the outer segment, so that light rays approaching and reflecting off the inner segment wall at acute angles cannot reach the outer segment. This result held for cones in both the central fovea and on the foveal slope. Varying refractive indices and dimensions of inner and outer segments within reasonable limits did not alter the outcome.

If the funneling property of the inner segment does not work, the effective aperture of newborns' cones must be the outer segment itself. If the smaller size of the newborn eye is taken into account, the angular diameter of the effective collecting area, the outer segment, is approximately 0.35 arcmin. The dimensions required to compute this value are given in Table 1. The effective aperture of adult foveal cones is, of course, the inner segment and is approximately 0.48 arcmin.

We also calculated the average spacing of cones in the newborn and adult fovea from the data of Yuodelis and Hendrickson.[16] We assumed that newborn and adult foveal cones are arranged in a regular hexagonal lattice.[28] Table 2 shows average cone spacings and associated Nyquist limits. The values for newborns differ by factors of 1.8 and 4.0 from those for the 15-month-old infants and the adults, respectively.

The intercone distances and effective collecting areas listed in Table 1 were used to construct the receptor lattices shown in Fig. 3. The white bars represent 0.5 arcmin. The light gray areas represent the effective collecting areas, that is, the cone apertures. The effective collecting areas cover 65, 4, and 2% of the retinal patches for the adult central fovea, the newborn foveal slope, and the newborn central fovea, respectively. We refer to these values as cone coverages in the remainder of the paper. Clearly, if the above assumptions are correct, the vast majority of incident quanta are not collected within newborn cone apertures.

Table 2. Nyquist Limits[a]

Source of Measurement	D (arcmin)	Nyquist Limit (cycles/deg)
Neonate central fovea	2.30	15.1
Neonate foveal slope	1.66	20.9
15-month central fovea	1.27	27.2
Adult central fovea	0.58	59.7

[a] Assuming a regular hexagonal lattice, the Nyquist limit in cycles per degree is $60/(\sqrt{3}D)$, where D is the center-to-center distance (in minutes of arc).

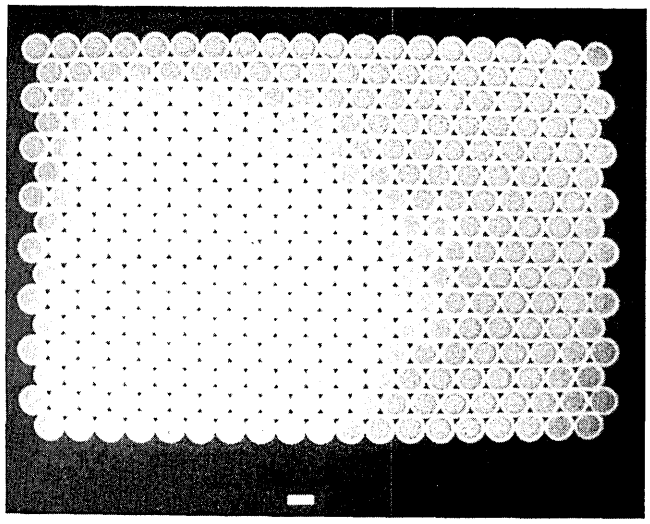

(a)

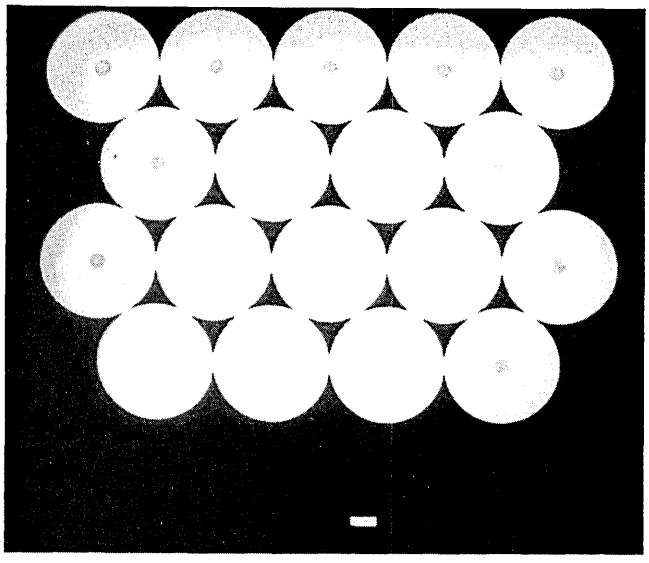

(b)

Fig. 3. Schematics of the receptor lattices used in (a) neonatal and (b) adult ideal observers. The white bars represent 0.5 arcmin. Light gray areas represent the inner segments; dark gray areas represent effective collecting areas. The effective collecting areas cover 65% of the adult central fovea but only 2% of the newborn central fovea.

The next factor that we considered is the efficiency of the outer segment. As shown in Figs. 1 and 2, the lengths of newborn and adult outer segments differ substantially. In the central fovea, for instance, the ratio of adult to newborn outer segment lengths is approximately 16:1. We assumed that neonatal and adult outer segments differ only in their widths and lengths (that is, that the concentrations and extinction coefficients of photopigment are the same). The critical equations and relevant parameters are given in Table 3. By our calculations, the 16:1 difference between adult and newborn outer segment lengths produces approximately a 10:1 difference in the number of isomerizations for a given number of incident quanta. The newborn outer segments are a bit longer on the foveal slope, so the corresponding ratio of adult to neonatal isomerizations is slightly lower for that part of the retina. These calculations imply that once quanta are delivered to outer segments, newborn cones are much less efficient than mature cones in producing isomerizations.

Taking into account the age-related changes in the factors listed in Table 1, we estimate that the adult central foveal cone lattice absorbs 350 times more quanta than does the newborn central foveal lattice. Stated another way, if identical patches of light are presented to newborn and adult eyes, roughly 350 quanta are effectively absorbed in adult foveal cones for every quantum absorbed in newborn cones.

We built an ideal observer for the adult central fovea and two neonatal ideal observers, one for the foveal slope and one for the central fovea. The properties built into these observers are listed in Table 1. All the ideal observers had three receptor types, short-, middle-, and long-wave-sensitive (SWS, MWS, and LWS, respectively) cones, with adult spectral sensitivities[29] in a ratio of 1:16:32.[30,31] We used Geisler's SDE software[8] to compute the performances of these observers for various spatial and chromatic tasks.

3. SPATIAL VISION

A. Contrast Sensitivity

We begin our analysis by considering the contrast sensitivity function (CSF). Before discussing development, however, we briefly discuss how optics and photoreceptor efficiency affect contrast sensitivity in adults. Banks and colleagues[32,33] calculated the contrast sensitivity of the adult ideal observer described in Table 1. These calculations represent the highest contrast sensitivity that the human adult fovea could have, gien quantal fluctuations in the stimulus; adult optics; and the size, spacing, and efficiency of adult foveal cones. Banks and colleagues also included con-

Table 3. Outer Segment Efficiency

Source of Measurement	Specific Axial Density	Outer Segment Length (μm)	Relative Number of Isomerizations	Ratio to Adult Value	Square Root of Ratio
Neonate central fovea	0.009	3.1	0.062	11.5	3.4
	0.014		0.095	9.0	3.0
Neonate foveal slope	0.009	4.6	0.091	7.8	2.8
	0.014		0.138	6.2	2.5
15-month central fovea	0.009	22.5	0.373	1.9	1.4
	0.014		0.516	1.7	1.3
Adult central fovea	0.009	50.0	0.712		
	0.014		0.855		

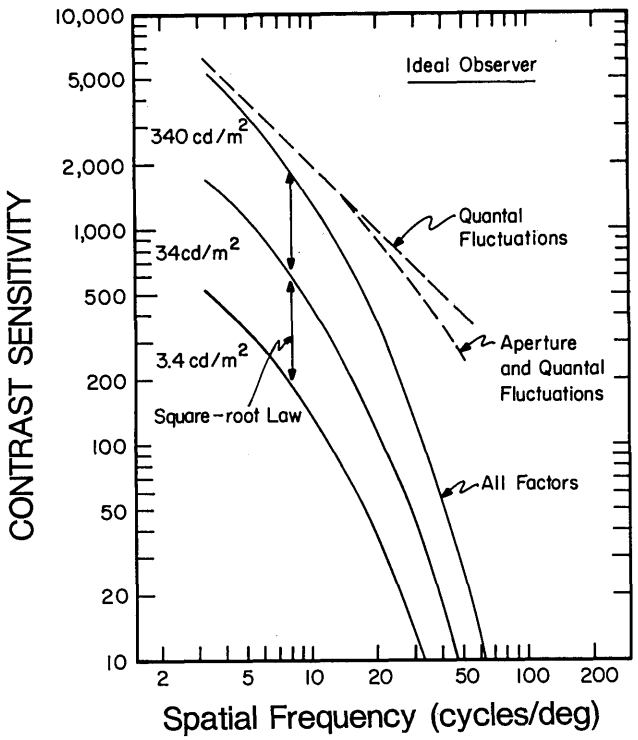

Fig. 4. CSF of an ideal observer incorporating different properties of the human adult fovea. Contrast sensitivity is plotted against the spatial frequency of fixed-cycle sine-wave grating targets. The highest dashed curve shows the contrast sensitivity of an ideal machine limited by quantal noise, ocular media transmittance, and photoreceptor quantum efficiency. The slope of −1 is dependent on the use of sine-wave gratings of a constant number of cycles. Space-average luminance is 340 cd/m^2. The lower dashed curve shows the contrast sensitivity with the receptor aperture effect added in. Finally, the highest solid curve shows the sensitivity with the optical transfer function added. The other solid curves represent the contrast sensitivities for 34 and 3.4 cd/m^2 (from Ref. 32).

siderations of a postreceptoral factor: the functional summation area for gratings of different spatial frequencies.[34]

Figure 4 displays the CSF of the ideal adult observer for sine-wave gratings of a constant number of cycles.[35] Different functions illustrate the contributions of various factors. The function labeled Quantal Fluctuations represents the performance of an ideal machine with no optical defocus and arbitrarily small and tightly packed photoreceptors. This function has a slope of −1, which means that contrast sensitivity is inversely proportional to patch width. The inverse proportionality is a manifestation of the square-root behavior of ideal machines.[10,11] Because Banks *et al.*[32] considered gratings of a constant number of cycles, the target area (and hence the number of quanta in the patch) was inversely proportional to the spatial frequency squared. The function labeled Aperture and Quantal Fluctuations represents performance when the photoreceptors are given the dimensions of adult foveal cones; comparing it with the one above it reveals the contribution of the receptor aperture effect. Notice that the attenuation caused by the receptor aperture is small. The solid curves represent performance with all factors included; the difference between this function and the one above it represents the contribution of optical defocus. The other solid curves represent contrast sensitivities at various luminances. As expected for ideal machines, these functions follow square-root law: reducing luminance by a log unit produces a half-log-unit reduction in contrast sensitivity.

Banks *et al.*[32] found that contrast sensitivity values for real adult observers were substantially lower than those of the ideal observer.[36] However, the shapes of the ideal and real CSF's were quite similar from 5 to 40 cycles/deg. The similarity of shapes demonstrates that the high-frequency rolloff of the adult foveal CSF can be explained by the operation of optical and receptoral factors plus the summation area of postreceptor detection mechanisms. This observation implies in turn that neural efficiency is constant from 5 to 40 cycles/deg for adult foveal vision. Banks *et al.*[32] also found that the luminance dependence of intermediate- and high-frequency sensitivities is similar in real and ideal adult observers, which means that adults exhibit square-root behavior. These observations are important to our analysis of contrast sensitivity development: the fact that the sensitivities of real and ideal adult observers vary in the same way with changes in spatial frequency and luminance legitimizes comparisons of performances of ideal and real observers at different ages.

We now consider the development of contrast sensitivity. Figure 5 displays neonatal and adult CSF's.[37–39] Contrast

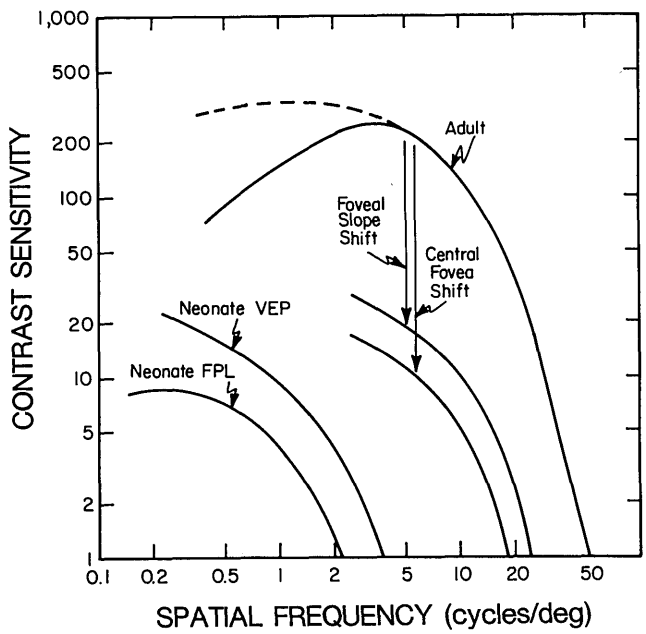

Fig. 5. Empirically determined adult and infant CSF's and the predicted loss of sensitivity caused by optical and receptoral factors. The curve labeled Neonate FPL is from Ref. 39 and was collected at 55 cd/m^2. The curve labeled Neonate VEP is derived from data from Ref. 37. The VEP data were collected at a space-average luminance of 220 cd/cm^2, so we shifted the function downward by 0.32 log unit to indicate its expected location at 50 cd/m^2 (under the assumption that square-root law holds). The curve labeled Adult represents data from Ref. 38 that were collected at 50 cd/m^2. Each vertical arrow represents the ratio of the ideal neonate sensitivity to the ideal adult sensitivity at each spatial frequency. The reductions in contrast sensitivity indicated by the arrows represent the effects of smaller image magnification, coarser spatial sampling by the cone lattice, and less-efficient photoreception in the neonate. The curves at the bottom of the arrows are the CSF's that one would expect if adult and neonatal visual systems were identical except for the preneural factors listed in Tables 1 and 3.

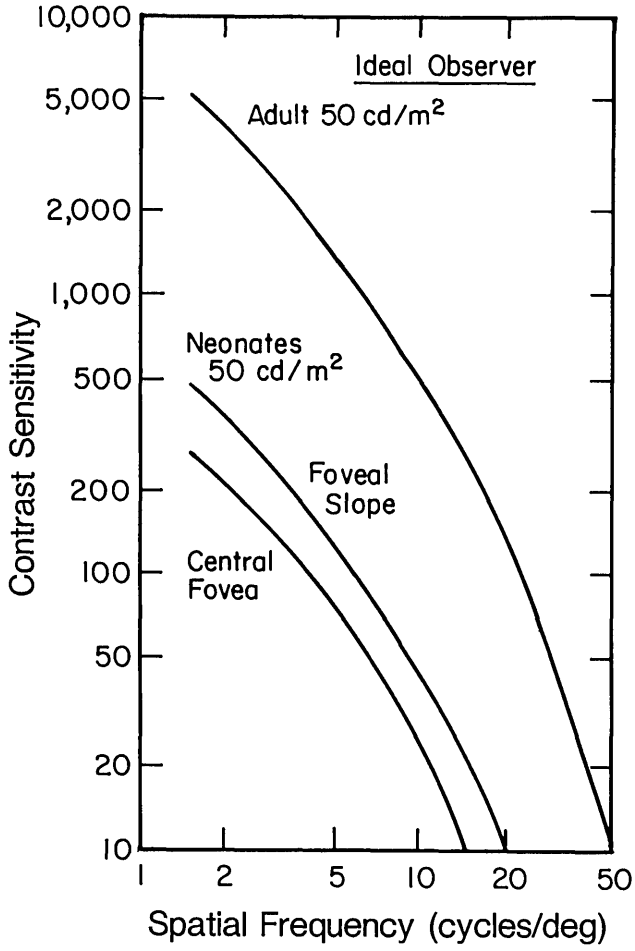

Fig. 6. CSF's for ideal observers incorporating the preneural factors of the adult and neonatal central foveas and the neonatal foveal slope. As in Fig. 4, the stimuli were grating patches of a constant number of cycles, in order to incorporate changes in summation area with spatial frequency.[32,34] Space-average luminance is 50 cd/m². The differences between adult and neonatal sensitivities are due primarily to the reduced quantum capture of the neonate's cone lattice.

sensitivity is obviously quite low in newborns, peak sensitivity being substantially lower than that of adults, whether it is measured by preferential looking (FPL)[22,39] or by visual evoked potential (VEP).[37,40] One can also see that visual acuity in neonates is quite limited, being roughly 25 times worse than that of normal adults.[41,42] As is commonly observed in studies with infants, VEP estimates of sensitivity are higher than FPL estimates, but the disparity at this age is not large.

To examine the extent to which the development of contrast sensitivity can be explained by optical and receptoral maturation, we computed the CSF's of the ideal neonatal and adult observers for fixed-cycle gratings. The ideal-observer CSF's are shown in Fig. 6. As in Fig. 4, these functions reflect performance limitations imposed by quantal fluctuations in the stimulus; by ocular media transmittance; by optical transfer; and by the aperture, efficiency, and spacing of photoreceptors. Notice that ideal sensitivity is higher at the margin of the newborn's foveola than in the center because of the greater efficiency of the foveal slope cones (Tables 1 and 3).

The differences between ideal adult and ideal neonatal contrast sensitivities are substantial. For example, the ratio of adult sensitivity to neonatal central foveal sensitivity at 5 cycles/deg is approximately 19:1 (1.3 log units). The major cause of the lower sensitivity in the newborn is the smaller quantum capture of its cone lattice. The CSF's of the neonatal and adult ideal observers are similar in shape for two reasons. First, the major determinant of shape, for gratings of a constant number of cycles, is optical transfer, and we assumed that neonates have adultlike OTF's. Second, although the receptor aperture is smaller in the neonatal observers, its effect on shape is trivial.

Can these predicted differences in sensitivity explain the differences observed between real adult and real newborn performances? If the visual systems of newborns and adults were identical except for the observed differences in eye size and in cone characteristics, one would expect the neonatal CSF to be a shifted version of the adult CSF. To examine this possibility, we compared empirically determined adult and newborn CSF's. Figure 5 shows an adult CSF at 50 cd/m² along with neonatal CSF's obtained at similar luminances with FPL and VEP. The vertical arrows indicate the amount of shifting that one would expect if the visual systems of adults and newborns were identical except for the optical and receptoral factors listed in Table 1. The shifts are vertical because our analysis involves the computation of the difference between the best-possible newborn and adult contrast sensitivities, spatial frequency by spatial frequency. As mentioned above, the fact that ideal and real adult contrast sensitivities are affected in similar ways by changes in spatial frequency and luminance makes plausible the implicit assumption behind the vertical shifting. In keeping with this, the adult function was not shifted at frequencies below 3 cycles/deg because the CSF's of real and ideal adult

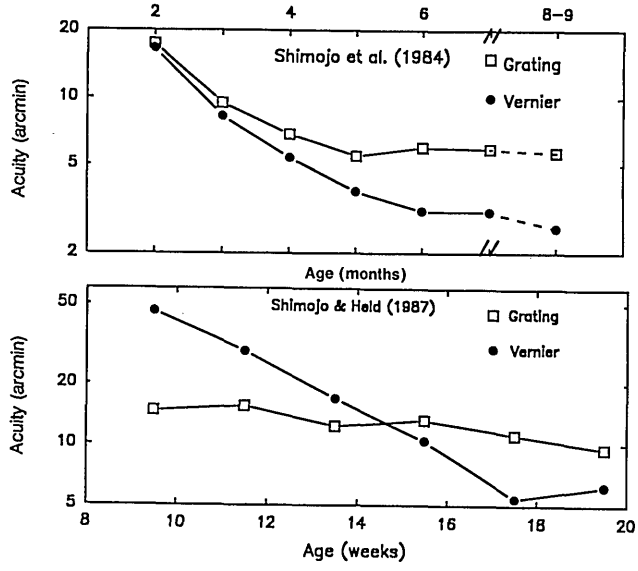

Fig. 7. Grating and vernier acuities as functions of age. The upper and lower panels illustrate data from Refs. 50 and 5, respectively. Acuity thresholds are plotted against age in weeks. Vernier thresholds are expressed as the just-detectable offsets in minutes of arc. Grating thresholds are expressed as the just-detectable stripe width in minutes. Thresholds in these experiments were measured by using the FPL procedure. High-contrast square-wave gratings were used for the grating experiments, and square-wave gratings with horizontal offsets were used for the vernier experiments.

observers are not similar in shape at low frequencies.[32,33] The shifting accounts for a substantial fraction of the observed newborn–adult disparity, but it does not account for all of it. Therefore additional factors must contribute to the newborn contrast sensitivity deficit. There are, of course, numerous candidates for these additional factors, including neural noise and poor motivation to respond. In the interest of simplicity, we shall call the gap between the real newborn CSF's and the shifted adult functions the postreceptoral loss. Our analysis suggests that the postreceptoral loss is approximately 7-fold (0.85 log unit) at 3 cycles/deg and 19-fold (1.3 log units) at 5 cycles/deg.[43]

A caveat is warranted before we conclude our discussion of contrast sensitivity. Despite the fact that the fovea subtends a large area at birth, newborns may use extrafoveal loci in contrast sensitivity experiments. Unfortunately, there are no quantitative data on the morphological development of extrafoveal cones, so it is possible that extrafoveal cones are actually more efficient than foveal cones at birth.[16,20] If this were the case, the disparity between predicted and observed contrast sensitivities (the postreceptoral loss) would be greater than indicated in Fig. 5.[44]

We conclude, within the assumptions of our analysis, that much of the spatial contrast sensitivity deficit observed early in life can be accounted for by immaturities in the morphology of foveal cones. The major constraint is the poor quantum catching and isomerization of the newborn's foveal cone lattice. These factors are, however, insufficient to explain the entire developmental gap, so subsequent stages in the visual process must be examined to explain the remainder.

B. Vernier and Grating Acuities

Several empirical observations suggest that mature vernier and grating acuities are limited by different neural mechanisms. For example, vernier acuity is disrupted more than grating acuity by amblyopia,[45] and it dissipates more rapidly with retinal eccentricity.[46,47] In fact, the eccentricity dependence of vernier thresholds correlates with the magnification of visual cortical modules, and that of grating thresholds correlates with the magnification of retinal ganglion cells.[46] In this section we examine optical and photoreceptor limitations on the growth of these two forms of acuity.

Photoreceptor spacing is a major limit to foveal grating acuity in adults. Specifically, acuity is similar to the Nyquist sampling limit of the foveal cone lattice.[23] In regard to development, Jacobs and Blakemore[1] argued that the Nyquist limit of the newborn monkey's foveal lattice is low enough to explain its relatively poor grating acuity. A similar relationship was not observed in newborn human infants (see Table 2 and Fig. 5). Although newborn Nyquist limits are much lower than those of an adult, they are not nearly so low as the highest grating acuities of 2–4 cycles/deg observed early in life.[41,42] Thus in human newborns the Nyquist sampling limit of the foveal cone lattice far exceeds the observed visual resolution.

The development processes of vernier and grating acuities were compared recently.[5,48–50] Figure 7 summarizes the results of the two most widely cited experiments. Vernier thresholds improved more rapidly with age than did grating thresholds. In fact, vernier acuity was actually poorer than grating acuity at the age of 9 weeks in one study.[5]

Shimojo and Held argued that the dissimilar growth curves for vernier and grating acuities reflect differing maturation rates of the mechanisms underlying these capabilities: "Differences between vernier acuity and grating acuity may be a reliable measure of the development of the central visual system because the contributions of peripheral visual processing, attention, and the response required of the infant are common in the two tasks and thus would not contribute to the difference." (See Ref. 50, p. 727.) In other words, the steeper ascent of vernier acuity may reflect rapid cortical maturation during the first half-year of life. This idea is reasonable because, as noted above, current theories

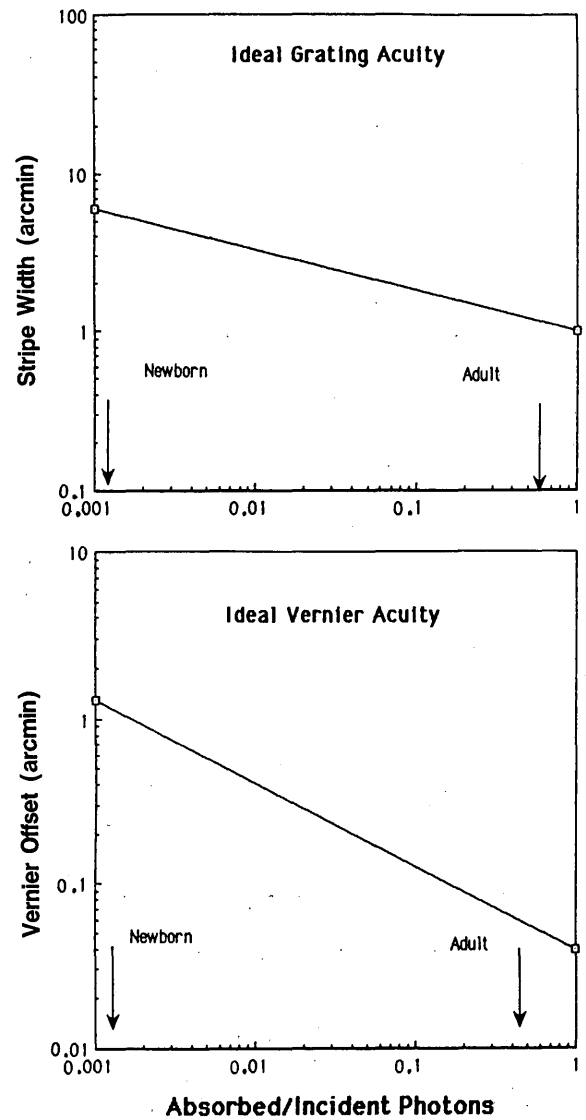

Fig. 8. Ideal grating and vernier acuity thresholds as a function of the proportion of incident photons absorbed. The stimuli were those of Ref. 5. Adult and newborn values are indicated by arrows. Space-average luminance was 100 cd/m^2, and target duration was 100 msec. We used different summation areas for the two tasks: 6 cycles × 6 cycles in the case of grating acuity[32,34] and 0.1 deg × 0.1 deg in the case of vernier acuity. The figure shows that ideal vernier thresholds are affected more by quantum efficiency than are ideal grating thresholds. These two results are manifestations of, on the one hand, the square-root relationship between the number of effective quanta and ideal vernier thresholds and, on the other hand, the roughly quarter-root relationship between quanta and ideal grating thresholds.

claim that vernier performance in adults correlates with the scale and the sensitivity of cortical modules and that grating performance correlates with the scale and the sensitivity of retinal neurons. In keeping with our theme, we examine the likely effects of immature optics and photoreception on early grating and vernier acuities.

As pointed out above, the major differences between the adult and neonate ideal observers are the superior light catching and spatial grain of the adult receptor mosaic, so an important question is how changes in efficiency might affect performance in different sorts of resolution tasks. Geisler[7] computed ideal-observer performance for two-dot separation and resolution tasks and found that separation acuity increased with the square root of efficiency and that resolution acuity increased with the quarter root of efficiency. The vernier and grating targets used in studies with infants are entirely different, however, so we calculated the performance of ideal observers with different efficiencies (one with that of the neonate, one with that of the adult, and so on) for typical stimuli. To this end, we used the stimuli of Shimojo and Held: high-contrast square waves for the grating acuity measurements and square waves with spatial offsets for the vernier acuity measurements. Details are given in the caption of Fig. 8, which shows plots of vernier and grating acuities as functions of the proportion of incident quanta effectively absorbed. The proportions absorbed for newborns and adults are indicated by the arrows. Ideal vernier thresholds are proportional to the square root of the number of effective quantum absorptions. Ideal grating thresholds rise more slowly with the number of absorptions. Because receptor efficiency improves significantly with age, these findings suggest that the gap between grating and vernier acuities is expected to expand developmentally from consideration of preneural limitations alone. The vertical positions of the curves are dependent on the assumed functional summation area (see the caption to Fig. 8). By manipulating the assumed area, we can produce functions that cross, such as those of Shimojo and Held. We do not plot these functions, however, because they are dependent on untested assumptions of effective summation areas.

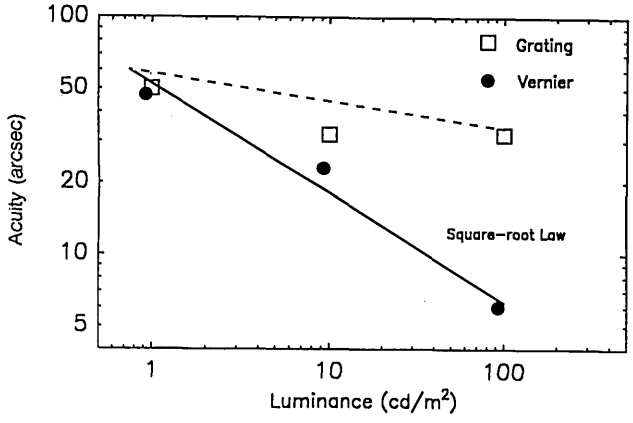

Fig. 9. Adult vernier and grating acuities plotted against background luminance. The vernier acuity task was similar to that of Ref. 5 except that the spatial frequency of the grating was 6 cycles/deg. Vernier acuity, defined as the smallest visible offset, is represented by the filled circles. Grating acuity, defined as the half-period of the highest visible spatial frequency, is represented by the open squares. The grating data are from Ref. 4.

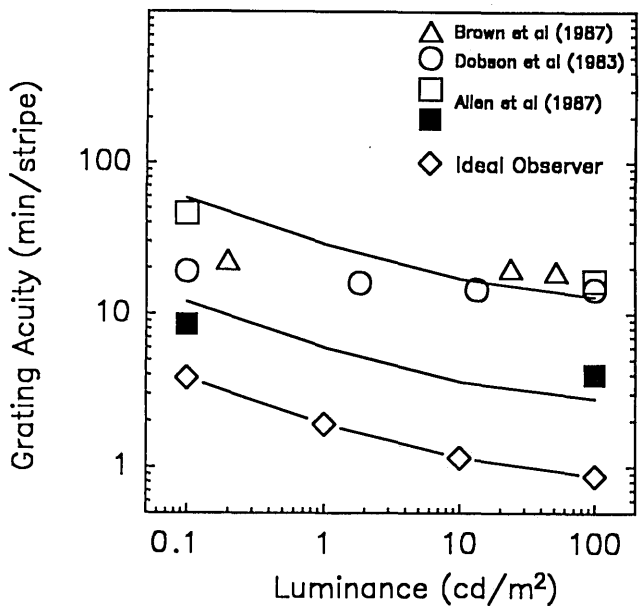

Fig. 10. Real and ideal infant grating acuity as a function of luminance. The circles, triangles, and squares are from three different experiments.[4,51] Open symbols represent data from FPL experiments, and filled symbols represent data from VEP experiments. The lowest solid curve represents the grating acuity of the neonatal ideal observer at various luminances. The other solid curves are shifted upward by 0.5 and 1.2 log units to facilitate shape comparisons.

Given the differing influences of quantum catch on ideal vernier and grating acuities, we next sought to determine whether real observers' acuities are affected in a similar fashion. To this end, we examined adults' vernier and grating acuities as functions of space-average luminance (see Fig. 9). There were no data in the literature on vernier acuity versus luminance for fixed contrast stimuli, so we made these measurements with the first author, an emmetropic adult, as the observer. The stimuli were identical to those used by Shimojo and Held[5] except that luminance was varied and the spatial frequency of the vernier grating was 6 cycles/deg. The observer viewed the targets monocularly with his natural pupil and best optical correction. A two-interval, forced-choice procedure was used. Target duration was 17 msec. (A short duration was needed in order to avoid apparatus limitations on the smallest displayable offset.) Thresholds were measured by varying the vernier offset according to the method of constant stimuli. Figure 9 displays the results. The grating acuities are from the adult data of Brown *et al.*[4] Notice that vernier thresholds followed square-root law and that grating thresholds exhibited a lesser dependence on luminance. The solid and dashed lines are the ideal observer's vernier and grating acuity thresholds, shifted vertically to fit the data. Clearly, real and ideal thresholds are affected similarly by changes in the number of quanta available for discrimination.

The luminance dependence of grating acuity has been examined in human infants, too.[4,51] Representative data are plotted in Fig. 10 along with the ideal-observer thresholds, which are shifted vertically for comparison. As do those of adults, the real and ideal thresholds of infants exhibit roughly similar dependences on the number of available quanta, although some of the data are shallower than

predicted. Thus the grating acuities of infants and ideal observers are affected similarly by changes in the number of quanta available for discrimination.

In summary, the behavior of ideal observers is consistent with reports that the growth curve is steeper for vernier than for grating acuity.[5,48–50] Consequently, the fact that these growth curves differ in slope does not necessarily imply anything about differing maturation rates among postreceptoral mechanisms. The quantitative fit between ideal performance and real performance is uncertain at this point because of the lack of information about spatial summation areas in children of different ages. It is therefore premature to assess whether maturation among preneural factors alone is sufficient to explain the relative development of vernier and grating acuities.

4. CHROMATIC VISION

Recent studies of the development of chromatic vision have sought to establish the youngest age at which infants can discriminate stimuli on the basis of hue alone and to characterize the nature of any observed color deficiencies.[6] Instead of reviewing all the recent work, we discuss only one set of experiments by Teller and colleagues. We have chosen these experiments for a combination of reasons. First, they are logically sound and elegantly conducted. Second, they involve young infants ranging from 4 to 12 weeks of age. Finally, they included luminance discrimination measurements, the importance of which will be evident later in this paper.

Teller and colleagues wished to determine whether young infants can make hue discriminations when brightness cues are eliminated and whether their pattern of discriminations is consistent with color-defective, dichromatic vision or color-normal, trichromatic vision. Specifically, they examined neutral-point,[52,53] Rayleigh,[54,55] and tritan[56] discriminations. In each study, discrimination performance was assessed by using the FPL procedure. Most of the studies included luminance and chromatic discrimination measurements. In luminance measurements, the targets were luminance increments or decrements on an otherwise uniform field. In chromatic measurements, the test targets were various hues presented in a series of luminances spanning adult heterochromatic brightness matches. The stimulus conditions and ages tested are listed in Table 4.

The chromaticities of the test targets and surrounds used in the neutral-point experiments[52,53] of Teller and colleagues are plotted in Fig. 11. Eight-week-old infants demonstrated that they can discriminate many, but not all, colors from white. They responded reliably to broadband red, orange, some greens, blue, and some purples. They did not, however, show that they could differentiate broadband yellow, yellow-green, one green, and some purples from white. Thus 8-week-old infants seemed to exhibit a neutral zone running from short wavelengths to yellow and green. Teller *et al.*[53] argued from these results that 8-week-old infants either have a tritan defect (tritanopia or tritanomalous trichromacy)[57] or are trichromats who fail to distinguish poorly saturated colors from white.

Adams and Maurer[58] also used a neutral-point-like test to study chromatic development. They reported that newborn and 4-week old infants distinguish a variety of broadband lights from white, but their data were unconvincing because of methodological shortcomings.[58]

Varner *et al.*[56] examined discriminations along a tritanopic confusion line. Table 4 lists the conditions. Eight-week-old infants distinguished a 416-nm light from a 547-nm surround at all relative luminances, so they do not appear to have a tritanlike deficiency. Four-week old infants, in contrast, did not discriminate between the two lights reliably, leaving open the possibility that they are tritanopic or tritanomalous.

In the Rayleigh discrimination experiments,[54,55] Teller and co-workers examined the ability of 4- to 12-week-old infants to discriminate long-wavelength lights. The stimulus conditions are described in Table 4. The surround was a narrow-band yellow. For luminance discrimination measurements, increments or decrements of the same yellow light were presented. For chromatic discrimination, either a narrow-band green or a broadband red was presented at one of a variety of luminances. The results were clear-cut. Most 8-week-old and essentially all 12-week-old infants reliably discriminated red and green from yellow, clear evidence that most infants in that age range do not exhibit deutan or protan defects. In contrast, the majority of 4-week-old infants did not make either discrimination, leaving open the possibility that they have deutan or protan defects. Packer *et al.*[55] also found a significant effect of target size. Twelve-week-old infants were able to make Rayleigh discriminations with 4- and 8-deg targets but not with 1- and 2-deg targets.

Teller and colleagues drew the following conclusions from these data. First, most infants are probably trichromatic by 12, if not 8, weeks of age; that is, they probably have three functional cone types and the postreceptoral machinery required to preserve and compare their signals. Second, at 4 weeks of age, the majority of infants may be color defective because most fail to make both Rayleigh and tritan discriminations. Teller and co-workers argued that younger infants' discrimination failures may be due to the absence or immaturity of receptoral or postreceptoral channels.

In sum, there are still no rigorous demonstrations that the majority of neonates can make hue discriminations. The absence of such evidence is consistent with the hypothesis that human neonates are generally color deficient. In the same vein, the postnatal development of chromatic vision may hinge on the maturation of chromatic mechanisms (e.g., the differential functional emergence of another cone type or of opponent color mechanisms). There is, however, another possibility. Perhaps neonates have a full complement of cone types and the requisite neural machinery to preserve and compare their signals, but their overall visual efficiency is simply too poor to allow them to demonstrate their chromatic capabilities. Similarly, older infants may exhibit reliable chromatic discrimination because of increased visual efficiency. In keeping with the key assumptions, we call this the visual efficiency hypothesis. We define visual efficiency as the discrimination performance of a visual system limited by optical and photoreceptor properties (Tables 1 and 3) plus a general postreceptoral loss. This definition is elaborated below. The remainder of this section is devoted to evaluating the visual efficiency hypothesis. We do so by determining whether age-related changes in chromatic discrimination can be explained by an analysis of the informa-

Table 4. Results and Predictions for Color Experiments of Teller and Colleagues

Experimenters	Age (weeks)	Task	Stimulus	Result[b]	Ratio	Predicted Weber Fraction	Accurate Prediction
Hamer *et al.*[54]	4	Chromatic	Red (633 nm)[a] on yellow (589 nm)	Fail	3.49	1.92	+
			Green (550 nm) on yellow	Fail	3.14	1.73	+
	8	Chromatic	Red[a]	Marginal	3.49	1.27	+
			Green	Marginal	3.14	1.13	+
	12	Chromatic	Red[a]	Pass	3.49	0.63	+
			Green	Pass	3.14	0.57	+
Packer *et al.*[55]	4	Intensity	Yellow (589 nm) (8° × 8°)	Threshold = ±0.27			
		Chromatic	Red (650 nm) (8° × 8°)	Fail	3.49	1.61	+
		Intensity	Yellow (4° × 4°)	Threshold = ±0.35			
		Chromatic	Red (4° × 4°)	Fail	3.49	1.92	+
		Intensity	Yellow (2° × 2°)	Threshold = ±0.55			
		Chromatic	Red (2° × 2°)	Fail	3.49	2.51	+
	12	Intensity	Yellow (8° × 8°)	Threshold = ±0.11			
		Chromatic	Red (8° × 8°)	Pass	3.49	0.54	+
		Intensity	Yellow (4° × 4°)	Threshold = ±0.18			
		Chromatic	Red (4° × 4°)	Pass	3.49	0.63	+
		Intensity	Yellow (2° × 2°)	Threshold = ±0.31			
		Chromatic	Red (2° × 2°)	Marginal	3.49	1.08	+
		Intensity	Yellow (1° × 1°)	Threshold = ±0.40			
		Chromatic	Red (1° × 1°)	Fail	3.49	1.40	+
Peeples and Teller[52]	8	Intensity	White (2800K) (14° × 1°)	Threshold = ±0.12			
		Chromatic	Red (633 nm)[a] on white	Pass	2.58	0.62	+
Teller *et al.*[53]	8	Intensity	White (2800K) (14° × 1°)	Threshold = ±0.12			
		Chromatic	Red (633 nm)[a] on white	Pass	2.58	0.62	+
			Orange (~611 nm)	Pass	4.13	1.00	+
			Yellow (~585 nm)	Marginal	12.26	2.95	+
			Greenish-yellow (~561 nm)	Fail	7.10	1.71	+
			Yellowish-green (~538 nm)	Fail	4.17	1.01	+
			Green 1 (~512 nm)	Marginal	3.29	0.79	−
			Green 2 (~516 nm)	Pass	3.23	0.78	+
			Greenish-blue (~496 nm)	Pass	2.90	0.70	+
			Blue (~486 nm)	Pass	2.52	0.61	+
			Bluish-purple	Pass	7.35	1.78	−
			Purple 1	Fail	10.32	2.49	+
			Purple 2	Marginal	9.94	2.39	+
			Reddish-purple	Pass	3.42	0.83	+
Varner *et al.*[56]	4	Intensity	Green (547 nm) (4° × 4°)	Threshold = ±0.16			
		Chromatic	Violet (416 nm) on green	Fail			−
	8	Intensity	Green	Threshold = ±0.10			
		Chromatic	Violet	Pass			+

[a] Wratten 29.
[b] Values for thresholds are given in log units.

tion content of the stimuli, the operation of preneural factors, and a measure of visual efficiency.

To introduce our approach, we first discuss luminance and chromatic discrimination in the mature visual system. Several investigators measured adults' luminance and chromatic CSF's.[59,60] Mullen,[59] for instance, measured luminance contrast sensitivity with monochromatic gratings of various spatial frequencies and chromatic contrast sensitivity with isoluminant red–green and blue–yellow gratings. She defined chromatic contrast as the Michelson contrast of the two components of each isoluminant grating. We adopt this definition throughout the remainder of this section. By this definition, luminance contrast sensitivity exceeded chromatic sensitivity by a factor of 4–5 for spatial frequencies above 2 cycles/deg. At lower frequencies, the luminance–chromatic difference diminished and finally reversed. An important question is whether reduced chromatic contrast sensitivity at intermediate to high spatial frequencies[59,60] reflects reduced sensitivity among postreceptoral chromatic channels as opposed to luminance channels or whether it simply reflects reduced cone contrast[61] caused by the overlapping spectral sensitivities of different cone types.

To address this question, Geisler[8] computed the performance of an adult ideal observer for the conditions of Mullen's experiment. The observer had LWS, MWS, and SWS cones in a ratio of 32:16:1. Geisler's ideal observer used cone outputs only. Consequently, any differences between ideal luminance and chromatic CSF's must be caused by information loss at the level of effective quantum capture in the cones. Naturally, the contrast sensitivity of the ideal observer was much higher than the sensitivity of Mullen's observers, but the effects of spatial frequency and chromatic

versus luminance contrast were quite similar.[62] To wit, the shapes of real and ideal luminance CSF's and real and ideal chromatic CSF's were nearly identical above >2 cycles/deg. Moreover, ideal luminance sensitivity was consistently 3.5 times greater than ideal chromatic sensitivity (using Mullen's definition of chromatic contrast) for the colors chosen. Geisler concluded therefore that the contrast sensitivities of real and ideal adult observers are affected similarly by the spatial-frequency and chromatic contents of the stimulus. No special weaknesses among chromatic mechanisms are needed, then, to explain sensitivity losses at isoluminance for intermediate to high spatial frequencies. This does not mean that postreceptoral chromatic mechanisms, such as color-opponent cells,[63] are not involved in chromatic contrast sensitivity tasks. Rather, Geisler's observation simply suggests that there is no significant information loss in signals transmitted through such chromatic mechanisms relative to signals transmitted through luminance channels.

Why is the ideal observer's sensitivity poorer for an isoluminant chromatic grating than for a luminance grating? The main cause is the extensive spectral overlap of cone photopigments and consequent reduced spatial modulation among cone signals for isoluminant gratings.[64] The diminished cone modulation at isoluminance is bound to reduce

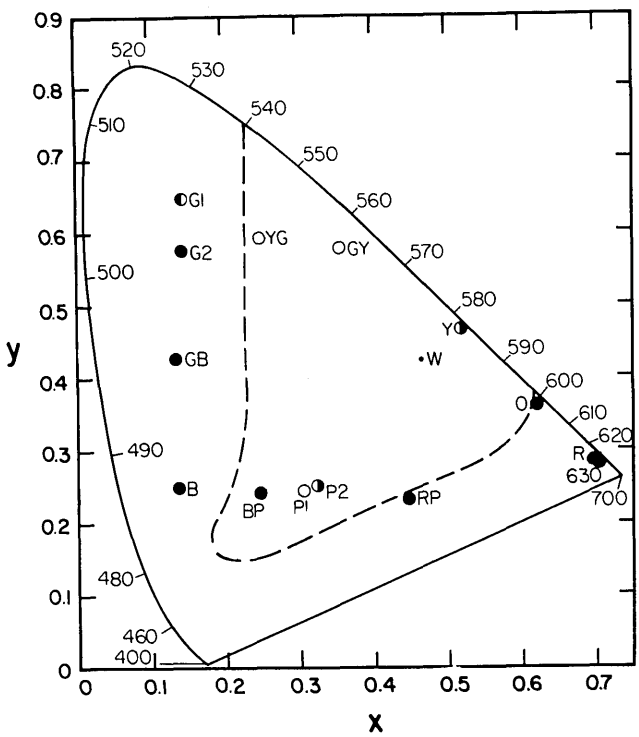

Fig. 11. Chromaticities of the stimuli used in the neutral-point experiments of Refs. 52 and 53. Subjects in both experiments were 8-week-old infants. Filled symbols represent stimuli that all infants reliably discriminated from white (W); open symbols represent hues that all infants failed to discriminate from white; half-filled symbols represent hues that some, but not all, infants discriminated from white. The dashed curve represents the boundary between hues that should and should not be discriminated from white according to the visual efficiency hypothesis. Hues falling outside the triangular area bounded by the dashed curve should be discriminable from white, and those falling within the area should not.

ideal sensitivity because ideal observers utilize all the information in the matrix of cone signals. The fact that real observers show similar sensitivity losses over a wide range of spatial frequencies suggests that the extensive spectral overlap of cone types is indeed a major constraint on human adult chromatic-contrast sensitivity.

We adapted the ideal-observer analysis to determine whether the visual efficiency hypothesis is consistent with empirical observations of early chromatic vision and its development. We first computed the sensitivity of the infant ideal observer for the experimental conditions of Teller and colleagues. The observer was identical to the one described in Table 1. In keeping with our hypothesis that young infants have a normal complement of cone types, we built in SWS, MWS, and LWS cones.[65] There are no data on the relative number of cone types at different ages, so we assumed an adultlike ratio of 1:16:32.[31] We also assumed that the cone pigments had adultlike absorption spectra.[29,66,67] The transmittance of the ocular media was again set to presumed neonatal values.

After constructing the infant ideal observer, we encoded the spectral characteristics of each stimulus and computed associated quantum catches of each cone type. This allowed us to compute the infant ideal observer's thresholds for the luminance and chromatic discrimination tasks listed in Table 4.[68] We expressed the ideal luminance discrimination threshold as the just-detectable luminance decrement ($d' = 0.96$) divided by the surround luminance.[69] To compute ideal chromatic discrimination performance, we constructed a stimulus composed of the uniform surround, a decrement in the surround, and an increment of the appropriate color. For example, the computer version of a Rayleigh stimulus[54,55] consisted of a uniform yellow surround (589 nm) and a square region of the same luminance with a 589-nm decrement and a broadband red (dominant wavelength, 630 nm) increment. With the magnitude of the 589-nm decrement fixed, we added the increment in various proportions around the presumed equiluminance point in order to find the luminance ratio for which the computed threshold was highest. The highest threshold was always at or close to equiluminance.

In the second stage of calculation, we manipulated the magnitudes of the decrement and the increment while maintaining equiluminance (that is, the decrement/increment ratio yielding the highest threshold), in order to establish the ideal observer's chromatic discrimination threshold. This threshold was expressed as a Weber fraction: the magnitude of the surround decrement (in this example, the yellow decrement) divided by the surround luminance. This definition of threshold is similar to that of Mullen.[59] Finally, we computed the ratio of the ideal Weber fraction for chromatic discrimination divided by the ideal Weber fraction for luminance discrimination. This ratio represents the theoretical disparity between luminance and chromatic discrimination thresholds, if it is assumed that performance is limited by preneural factors only. Stated another way, it is the threshold ratio that one would expect if there were no information loss among postreceptoral mechanisms or if the information loss were similar for the channels used in luminance and chromatic discriminations. The ratios for each age group and experimental condition are given in Table 4. Higher ratios mean higher chromatic thresholds. The ratios vary

widely from 2.52 for blue-on-white discrimination to 12.3 for yellow-on-white discrimination. These ratios, by the way, do not depend on assumptions about spatial summation or on the part of the retina that neonates use in chromatic tasks.[70]

The ideal observer's luminance discrimination thresholds were much lower than those of Teller's infants. Furthermore, the neonate ideal observer was able to make all the chromatic discriminations when the contrast of the target (surround decrement/surround luminance ratio) was 1.0, as it was in Teller's experiments. Thus, as in the spatial tasks discussed in Section 3, the ideal observer exhibited notably better performance than did real neonates. In Section 3 we attribute this performance disparity to postreceptoral losses, which reflect in part the ideal observer's ability to sum information perfectly across space, which human infants and adults do not.

The visual efficiency hypothesis outlined earlier in this section states that young infants' inability to make chromatic discriminations is a manifestation of low visual efficiency in general rather than some deficit among chromatic mechanisms *per se*. For the purposes of this hypothesis, we define visual efficiency as the discrimination performance of a visual system limited by optical and photoreceptor properties (Tables 1 and 3) plus a general postreceptoral loss. We, of course, do not have an explicit measure of the postreceptoral loss, so Teller's empirically determined luminance discrimination thresholds are used. In this way, the efficiency hypothesis states that the ratio of infants' chromatic discrimination thresholds divided by their luminance discrimination thresholds should be similar to the ratio of the neonatal ideal observer's chromatic thresholds divided by its luminance thresholds. According to hypothesis, then, luminance and chromatic sensitivities should follow similar growth curves. Predictions of the visual efficiency hypothesis are obtained by multiplying the observed luminance discrimination thresholds (the Weber fractions measured by Teller and colleagues) by the ratio of the ideal chromatic threshold to the ideal luminance threshold. For an example, refer to Table 4. In the experiment of Packer *et al.*[55] the observed luminance discrimination threshold at 4 weeks was 0.27 log unit, a Weber fraction of 0.46. The ratio of ideal chromatic threshold to luminance threshold was 3.49. Thus the chromatic discrimination Weber fraction (or threshold contrast) predicted by the efficiency hypothesis is simply 0.46×3.49, or 1.61. But the contrast of Teller's stimuli (surround decrements replaced by increments of a different hue) were always, by our definition, 1.0. In the example, then, the hypothesis predicts a discrimination failure. The predicted thresholds vary with age, luminance, and target size because the reported luminance discrimination thresholds[52–56] varied with those factors. Consequently, the hypothesis makes the unsurprising prediction that chromatic discrimination improves with increasing luminance, target size, and age. The predictions varied with the colors of the target and surround, too, because the ratios of ideal chromatic threshold to ideal luminance threshold depended on the spectral composition of the stimuli. Thus some discriminations, such as that of yellow from white, are expected to be more difficult than others, such as blue from white.

The predicted Weber fractions for the neutral-point discrimination tasks[52,53] are given in Table 4. The visual efficiency hypothesis predicts discrimination failures for predicted Weber fractions greater than 1.0 and successes for smaller fractions. Figure 11 depicts the predictions and data in the format of the CIE chromaticity diagram. The data points represent the stimuli and the infants' performances. The dashed curve represents the predictions. Colors within the triangular area bounded by the dashed curve should, according to the hypothesis, be indiscriminable from white, and colors outside the area should be discriminated reliably. (The reader may recognize these as colorimetric purity discriminations.[71,72]) The zone of theoretically indiscriminable stimuli is broad. As expected, it does not resemble confusion lines for any standard dichromatic observer because the infant ideal observer had three cone types. Seven of the eight colors that were discriminated reliably fall outside the area bounded by the dashed curve, so performance is predicted correctly in those cases. The three colors that were not discriminated fall inside the bounded area, so predictions are accurate in those cases, too. There were three colors that were discriminated by some infants and not by others. Two fall within the bounded area and one does not. If we classify the marginal responses in those three cases as discrimination failures, then two of the three predictions are correct. Given that assumption, the efficiency hypothesis predicts 12 of the 14 experimental results (or 11 of 14, if we classify marginal responses as reliable discrimination). We conclude that the performances of 8-week-old infants in Teller's neutral-point experiments[52,53] are largely consistent with the predictions of the visual efficiency hypothesis.

The predictions for the Rayleigh discrimination experiments[54,55] are also given in Table 4 and are illustrated in Figs. 12 and 13. Consider the experiment of Packer *et al.*[55] first. The ratio of the ideal chromatic threshold to the ideal luminance threshold was 3.49 for all conditions. Hence the efficiency hypothesis predicts that chromatic discrimination thresholds should consistently be 3.49 times higher than luminance discrimination thresholds. We again multiplied empirical measurements of luminance discrimination thresholds by the ratio of the ideal chromatic threshold to the ideal luminance threshold to estimate the Weber fractions that, according to the hypothesis, would be needed for reliable discrimination. These fractions are listed in Table 4 and plotted in Fig. 12. The dashed line represents chromatic contrasts of 1.0, the value presented by Packer *et al.*[55] All the fractions for 4-week-old infants are greater than 1.0, so the hypothesis predicts discrimination failures for all target sizes at that age. The data and predictions for 12-week-old infants are more complicated. The fractions are less than 1.0 for 4- and 8-deg targets, so for them the hypothesis predicts reliable discrimination. The fraction is slightly greater than unity for the 2-deg target, so a near miss is predicted. Finally, the fraction is well above unity for the smallest target, so a discrimination failure is predicted. The efficiency hypothesis therefore correctly predicts the results for all three conditions at 4 weeks and for all four conditions at 12 weeks.

The other Rayleigh discrimination experiment[54] did not include luminance discrimination measurements, so we adopted the luminance discrimination data of Packer *et al.*[55] (for 4-deg targets) because their conditions were similar. The 8-week value was assumed to be the average of the 4-

and 12-week thresholds of Packer *et al.* The ratios of the ideal chromatic threshold to the ideal luminance threshold were 3.49 for the red target and 3.24 for the green. Figure 13 displays the empirical observations and the predictions of the efficiency hypothesis. The dashed line again indicates the chromatic contrast of the experimental stimuli. The predicted Weber fractions are well above unity for 4-week-old infants, so the efficiency hypothesis correctly predicts clear discrimination failures for red and green targets at that age. The fractions are slightly greater than 1.0 for 8-week-old infants, so near misses are predicted. Finally, the fractions are well below unity for the oldest infants, so consistent discrimination is predicted correctly for both colors at that age.

The predictions of the visual efficiency hypothesis are consonant with the observed pattern of Rayleigh discriminations. The hypothesis assumes no deficit among chromatic mechanisms because the neonatal ideal observer has three functional cone types and uses optimal strategies to compare their outputs. Thus poor Rayleigh discrimination performance early in life does not necessarily imply deficiencies among chromatic mechanisms *per se*.

We next examine the performance of the infant ideal observer in the conditions of the tritan discrimination experiment.[56] Interestingly, the ideal observer's chromatic performance near isoluminance actually exceeded its luminance performance; that is, the threshold Weber fraction of the ideal observer was lower for discrimination of violet (416 nm) from green (547 nm) near isoluminance than for discrimination of a green decrement alone. This result was not dependent on the definition of isoluminance: the ideal Weber fraction was related monotonically to the proportion of violet light in the target. This behavior, which was not observed for any of the other color pairs that we examined, occurred because the ideal observer adopted a strategy in this chromatic task that was different from that used in the other tasks. The 547-nm surround stimulates MWS and LWS cones and not SWS cones. The 416-nm target, on the other hand, stimulates SWS cones quite favorably. In the luminance discrimination task, the ideal observer constructed a receptive field (a weighting function) that signaled the presence of the luminance decrement by detecting a decrease in the MWS and LWS cone inputs in the region of the target. SWS cones are not stimulated by a 547-nm surround, so their signals were not weighted in this decision. SWS cone signals were much more informative in the chromatic task, regardless of the relative luminance of the surround and test, because they are not driven by the surround. The ideal observer consequently adopted the optimal strategy of weighting SWS cone signals alone. Thus, whenever stimulation of SWS cones exceeded a rather low criterion, the ideal observer judged that the 416-nm target was present. This behavior suggests that information is in principle available at the photoreceptors of trichromatic observers to discriminate very-short-wavelength targets from long-wavelength surrounds more easily than simple luminance decrements in such surrounds.

Color-normal adults actually exhibit similar behavior in colorimetric purity experiments.[71] Smith *et al.*[72] provided a clear example. They measured the ability of adults to discriminate a mixture of a white light and a spectral light from a white field of the same luminance. They expressed their results as colorimetric purity thresholds $[L_\lambda/(L_\lambda + L_w)]$,

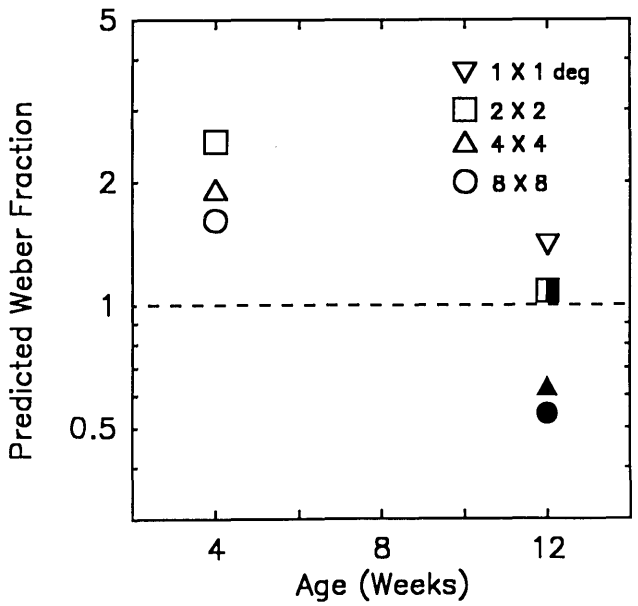

Fig. 12. Data and predictions for the experiment of Ref. 55. Predicted Weber fractions are plotted as a function of age in weeks. Open symbols represent conditions in which infants did not reliably discriminate red from yellow (see Table 4 for stimulus details). Filled symbols represent conditions in which infants exhibited reliable discrimination, and half-filled symbols represent conditions in which some infants exhibited reliable discrimination and some did not. Target size is indicated by the symbol conventions displayed in the upper right. The dashed line represents the contrasts of the stimuli presented in this experiment. The vertical placement of the various symbols corresponds to the Weber fraction predicted by the visual efficiency hypothesis. Thus symbols above the dashed line represent conditions in which discrimination failures are predicted, and symbols below the line represent conditions in which reliable discrimination is predicted.

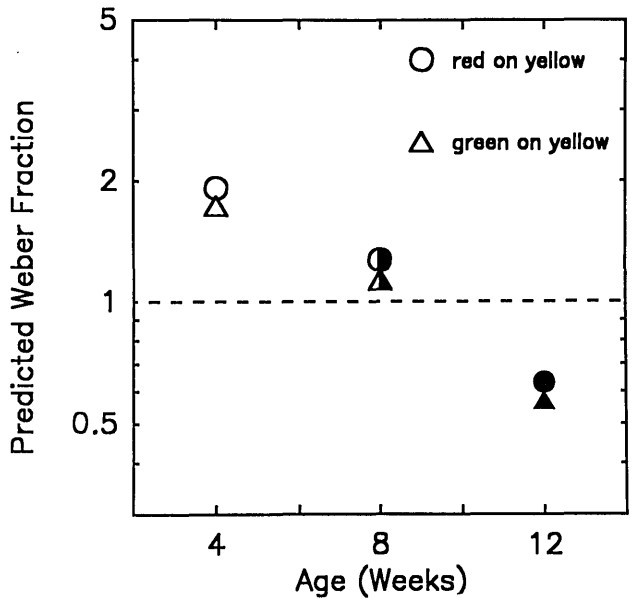

Fig. 13. Data and predictions for the experiment of Ref. 54. Conventions are as described for Fig. 12 except that the different symbol shapes represent green-on-yellow discriminations and red-on-yellow discriminations.

where L_λ and L_w are the luminances of the spectral increment and of the white surround once decremented, respectively. One can show that this expression is equivalent to the Weber fractions that we described earlier in this section. The chromatic Weber fractions in the experiment of Smith *et al.* varied from 0.27 (−0.57 log unit) for 570 nm to 0.0052 (−2.28) for 430 nm. The 430-nm-versus-white condition is similar to the chromatic condition in the infant tritan discrimination experiment[56] in that the target stimulates SWS cones much more than the surround does. Under similar conditions, Smith *et al.* obtained Weber fractions for luminance discrimination of 0.056 (−1.25 log units). Thus the threshold for discriminating a mixture of white and 430-nm light from an equiluminant white light was approximately a log unit lower than the luminance discrimination threshold.

The pattern of results in the infant tritan experiment was qualitatively different for the youngest infants. Four-week-old infants were less able to detect a short-wavelength target in a long-wavelength surround near isoluminance than when the short-wavelength target was dimmer than the surround. The behavior of 4-week-old infants therefore is quite different in this task from those of color-normal adults and ideal observers. Moreover, the visual efficiency hypothesis cannot account for the discrimination failures of 4-week-old infants in this experiment. These observations imply that young infants may well have a tritan defect: dysfunctional or insensitive SWS cones or inappropriate postreceptoral processing of their signals.

The results of the other experiments of Teller and coworkers are consistent with the hypothesis that neonates have a tritan defect but for trivial reasons. The only other discriminations tested at 4 weeks of age were Rayleigh discriminations that do not require information from SWS cones. We also wished to determine whether Varner's conclusion that SWS cones are functional at 8 weeks is consistent with other results. To this end, we built an infant ideal observer with MWS and LWS cones only. We recomputed for this observer the ratios of the chromatic threshold to the luminance threshold for the neutral-point studies.[52,53] As expected, the predictions for most chromatic discriminations changed little if at all. The only significant changes were the predictions for discriminating blue (B in Fig. 11), purplish-blue (PB), and purple (P1 and P2) from white. In each case, the efficiency hypothesis predicts that an observer with no SWS cones should find these discriminations more difficult. Figure 11 shows that 8-week-old infants failed in these discriminations anyway, so this reanalysis neither supports nor contradicts the hypothesis that SWS cones are functional by that age.

In summary, the predictions of the visual efficiency hypothesis are consistent with the pattern of Rayleigh and neutral-point discriminations observed by Teller and colleagues. The ideal observer used to evaluate this hypothesis has three functional cone types and uses optimal strategies to compare their outputs. Consequently, discrimination failures observed among the youngest infants and for small targets among the older infants do not necessarily imply deficiencies among chromatic mechanisms *per se*. Rather, the failures can be explained by an analysis of the information available at the photoreceptors of a trichromatic observer and changes in luminance discrimination capabilities alone. The predictions of the visual efficiency hypothesis are inconsistent with the tritan discrimination performance of 4-week-old infants.[56] We conclude therefore that young infants may in fact manifest some form of tritan defect.

5. DISCUSSION

In this section we compare our results with those of other investigators, relate our analyses and findings to the so-called dark glasses hypothesis, consider various hypotheses about the sources of the postreceptor loss, and discuss the sorts of visual tasks for which this sort of analysis is likely or unlikely to yield useful insights.

A. Comparisons with Wilson's Analysis

Wilson[2] concluded that immaturities among neonatal foveal cones are sufficient to explain the poor grating acuity of human newborns and the course of subsequent acuity development. In contrast, we concluded that front-end deficiencies alone account for only a fraction, albeit a large one, of the disparity between adult and newborn grating acuity. Our analyses differed in many ways despite the fact that we used the same anatomical data.

First, we estimated that 6–9% of quanta incident upon an outer segment in newborn central foveal cones are effectively absorbed (for an adult/newborn ratio of approximately 10), and Wilson, using a different approach, estimated 12% (a ratio of 7). Our method, which is based on a direct application of Beer's law,[67] probably provides a better estimate of outer segment efficiency.

Second, Wilson's estimate of newborn Nyquist limits (13.8 cycles/deg) differed slightly from ours (15.1 cycles/deg) because he assumed a square lattice and we assumed a triangular (or hexagonal) lattice.[28]

Third, Wilson's approach for linking photoreceptor properties to predicted performance was quite different from ours. He began with a quantitative model of spatiotemporal filters in the adult visual system[73] and then transformed the sensitivity and the spatial scale of these filters according to the traits of young foveal cones. Wilson considered two receptor properties and one neural property in transforming his filters: (1) changes in cone spacing were used to transform preferred spatial frequencies, (2) changes in cone density and outer segment efficiency were used to modify filter sensitivities, and (3) presumed changes in inhibitory connections among retinal and cortical neurons were used to transform filter bandwidths. Let us focus on the second assumption because it has rather large consequences. His means of adjusting mechanism sensitivities according to cone density and outer segment efficiency had quite different consequences from those of our adjustments to the adult ideal observer. In regard to cone density, Wilson transformed the spatial scale (the space constants) of each spatiotemporal filter by the ratio of adult cone spacing to infant cone spacing. He then divided the sensitivity parameter of his mechanisms by the square of the ratio of adult space constants to newborn space constants. The reasoning behind this manipulation is not given, but it reduces the amplitudes of the infant filters in the space domain by a factor of 22. (Note that this manipulation is not the same as the cone coverage factor that we discuss because Wilson did not compute the relative area of cone apertures.) The combination of large

reductions in filter sensitivity and scale that is assumed by Wilson produces a larger grating acuity loss than our analysis does.

In sum, much of the discrepancy in predictions stems from differing assumptions about how anatomical changes are likely to affect visual sensitivity. Wilson's approach is reasonable but makes many more assumptions than does ours.

B. Comparisons with the Analysis of Brown *et al.*

As we do for neonates, Brown *et al.*[4] rejected the hypothesis that the poor grating acuity of 2-month-old infants is explained by the reduced efficiency and sampling frequency of the foveal cone mosaic alone. To reach this conclusion, they used reasoning similar to ours in calculating age-related changes in numerical aperture, cone coverage, and inner and outer segment efficiencies. They concluded that the 2-month-old foveal cone lattice absorbs incident quanta at moderate photopic luminances at 1/14 to 1/55 the rate of the adult lattice. The corresponding figure for our neonatal lattice is much lower: 1/350. The discrepancy stems primarily from differences in the estimates of outer segment efficiency. Using Beer's-law equations,[67] we calculated the efficiency for newborn cones, and Brown *et al.* calculated it for 2-month-old cones. Consequently, they used much longer outer segments, derived by interpolating between values for newborns and 15-month-old infants,[16] in their calculations. They also assumed a slightly lower specific axial density. A secondary cause of the discrepancy in our calculations involves their assumption of a larger pupil diameter.[18]

C. Dark Glasses Hypothesis

We argue that the most important, but not the only, limitation to early spatial vision and chromatic vision is the lower effective quantum catch of the foveal cone mosaic. The lower catch is, in a sense, similar to the effect of reducing the retinal illuminance of the stimulus by placing dark glasses in front of the eye. This is the dark glasses hypothesis,[74] which, when adapted to development, states that the performances of infants and adults can be equated by increasing the light level presented to infants enough to overcome the attenuation of the theoretical glasses. According to this hypothesis, infant spatial and chromatic vision at a suitably bright light level should be similar to adult vision at a lower level. The dark glasses hypothesis is appealing for its simplicity, but it probably misrepresents the differences between neonatal and adult foveal cone lattices. To explain our reasoning, let us consider photoreceptor stimulation at two levels of analysis.

(1) Consider the total quantum catch at a given retinal illumination across the whole lattice. Because cone coverage and outer segment efficiency are much lower in neonates (Tables 1 and 3), the effective catch should be 1/350 that in adults. For tasks in which the total quantum catch across the lattice is a major limitation to performance, neonatal sensitivity should approach adult levels if the attenuating factors are overcome by increasing illumination 350-fold. This observation is, of course, consistent with the dark glasses hypothesis.

(2) Now, consider the consequences of varying retinal illuminance at the level of individual cones. In particular, consider the illumination required to bleach a fixed proportion of photopigment (assuming, again, that newborn and adult outer segments are equivalent except in length). For outer segments with lengths of 3.1 and 50 μm (Table 1), specific axial densities of 0.011 (Table 3), regeneration time constants of 120 sec, and photosensitivities of 3.5×10^6 Td-sec, the illuminance required to bleach half the photopigment would be 4.47 and 4.52 log trolands in newborns and adults, respectively.[75] Of course, the number of absorbed quanta across the receptor lattice would be much lower in neonates than in adults at these half-bleaching illuminances. Thus, despite the profound differences in the efficiencies of the two lattices, half-bleaching retinal illuminances should be similar in newborns and adults. Consider the consequences of this observation. At increasing light levels, a variety of adaptation mechanisms desensitize photoreceptors and retinal neurons in order to maintain discrimination capacity. The mechanisms include photopigment depletion and multiplicative and subtractive adjustments. In adults, photopigment depletion is a significant determinant of threshold at high luminances.[75] The similarity of half-bleaching constants across age implies that depletion would become significant at similar (but high) retinal illuminances in newborn and adult foveal cone lattices. This observation clearly runs counter to the dark glasses hypothesis. More importantly, if multiplicative and subtractive adaptive effects are related to the proportion of bleached photopigment, they too would start to affect performance at similar (and relatively low) retinal illuminances in newborns and adults, a circumstance that would also be inconsistent with the hypothesis.

In summary, the dark glasses hypothesis probably misrepresents the functional consequences of photoreceptor maturation once one considers the likely effects of adaptive changes in individual cones. Consequently, newborn performance in tasks limited by information at the photoreceptors may never achieve the adult levels observed at moderate luminances.

D. Contributors to the Postreceptor Loss

The performance of the neonatal ideal observer was much better than that of human neonates in all the tasks considered. This is hardly surprising given that human adult performance does not equal ideal performance in these same tasks. More interestingly, the gap between real and ideal newborn performance was always larger than the gap between real and ideal adult values. This means that neonates, although significantly limited by optical and receptoral deficiencies, use the information that is available at the photoreceptors less efficiently than adults do. What postreceptoral factors contribute to this additional developmental deficit? We consider some of the obvious candidates here.

(1) Before considering mechanistic explanations of the postreceptor loss, we should mention a methodological explanation: perhaps the sensitivity of the young visual system is actually better than we think, so that the postreceptoral loss is ascribed properly to motivational deficiencies. This hypothesis is difficult to evaluate because there is no theory of motivational deficiency. It is difficult therefore to know where to look for its effects. Motivational explana-

tions were evaluated and found lacking in previous studies,[41,76] so we will not elaborate here. It should be noted though that VEP estimates of neonatal contrast sensitivity and grating acuity still fall well short of the values predicted from front-end losses as plotted in Fig. 5; that is, whether one relies on behavioral or electrophysiological measurements of visual sensitivity, one cannot explain all the differences between neonatal and adult performance from front-end losses alone.

(2) The young visual system might sum information over smaller spatial and shorter temporal intervals than the mature system does. To understand how this would elevate threshold, consider the performance of a visual system identical to that of a neonate but with more-extensive spatial and temporal summation. Its threshold would be lower because it would be better able to use the information contained in the large, long-duration stimuli employed in infant experiments. This hypothesis is, however, inconsistent with data showing that spatial summation and temporal summation of infants are, respectively, more extensive than and similar to those of adults.[77]

(3) Finally, there is a broad range of explanations involving intrinsic noise and neural attenuation that might explain age changes in the postreceptoral loss. Signal-to-noise ratios determine threshold performance, so any process that adds noise or reduces signal degrades performance. There are numerous possibilities, so let us simply discuss one plausible example. Several pieces of evidence imply a variety of immaturities in the visual cortex of human neonates. These include psychophysical and electrophysiological demonstrations of the delayed emergence of orientation tuning, spatial-frequency tuning, symmetric monocular optokinetic nystagmus, and more.[78] Neurophysiological investigations have found similar deficits among cortical cells in young kittens.[79] A consistent and striking observation is that young cortical cells respond sluggishly compared with adult cells. Their response latency, fatigability, and peak firing rate are much lower than in mature neurons. The firing rates of retinal ganglion cells, in contrast, do not differ markedly across age.[80] The peak firing rate decreases at successive sites in the geniculostriate pathway of adult cats, but the effect is more dramatic in kittens. Reduced firing rates from retina to cortex, if caused by random or nearly random dropping of spikes from one cell to the next, decrease the total number of spikes in an unpredictable way. If spike trains are Poisson distributed or nearly so, a drop in the mean number of spikes reduces the signal-to-noise ratio. Thus successive reductions in firing rate, which appear to be prominent in the immature visual system, may well have the same effect as adding intrinsic noise: they decrease signal-to-noise ratios and consequently should elevate the threshold.[81]

E. Developmental Findings Suited and Unsuited for Ideal-Observer Analyses

According to Occam's razor, scientific explanations should be sought first in terms of known quantities. We have followed this philosophy by examining the information available at the photoreceptors for making a variety of spatial and chromatic discriminations and by calculating how that information changes with age. As it turned out, the differing growth curves of vernier and grating acuities are expected from an analysis of age-related changes in the information at the photoreceptors. Thus more complicated explanations involving different growth rates among retinal and cortical mechanisms[5] may not be required. We also found that the inability of neonates to make a variety of chromatic discriminations is consistent with analyses of the information at the receptors. Consequently, explanations involving delayed development of chromatic mechanisms[54] are not necessary, except for mechanisms involved in tritan discriminations.[56]

Only a subset of the spatial and chromatic tasks described in the literature on infants has been examined here. Indeed, the chosen tasks are ones in which real observers are most likely to behave in a manner similar to that of an ideal observer. This sort of analysis would be less informative for a number of other spatial and chromatic tasks. For example, spatial-frequency masking and orientation masking[82] occur at postreceptoral sites, so their development[78] would not be evident in ideal observers such as ours. As another example, increment-threshold functions follow Weber's law across a wide range of stimulus conditions.[10] The Weber's-law behavior is in part a manifestation of the operation of adaptation mechanisms, a factor not considered in this analysis. Consequently, an important aspect of the development of increment-threshold functions[83] is not reflected in age-related changes in front-end limitations. Finally, the sensitivity roll-off and Weber's-law behavior of the low-frequency end of the mature CSF[84] is attributed commonly to the operation of lateral interactions among retinal network mechanisms, another factor not considered here. Thus the development of this property of the CSF[22,39,85] also is not manifest in ideal-observer performance.

The development of numerous spatial and chromatic capabilities, therefore, is not evident in analyses of age-related changes in the information at the photoreceptors. Nonetheless, ideal-observer analyses such as ours might still be quite helpful in the investigation of such capabilities. As pointed out by Watson,[86] even departures of the performance of real observers from that of the ideal observer are important clues about the structure of processing. Such departures show that human visual performance is influenced substantially by postreceptoral sites. The magnitude and the character of the departures delineate what must be explained by postreceptoral processes. Similarly, developmental changes in the departures between real and ideal performances indicate how postreceptoral contributions vary with age.

6. SUMMARY

We examined the contributions of preneural factors to the differences between neonatal and adult spatial and chromatic vision. Ideal observers were constructed that incorporated the optics; the ocular media; and the photoreceptor aperture, efficiency, and spacing of adult and neonatal foveas. Comparison of the performance of these ideal observers allowed us to compute the contribution of optical and receptoral immaturities to deficits in the spatial and chromatic vision of neonates. Our three main findings were as follows:

(1) Immaturities in preneural mechanisms alone (primarily reduced eye size and changes in photoreceptor morphology) predict a 1.3-log-unit decrease in contrast sensitiv-

ity and a 2-octave decrease in grating acuity. Although these are substantial effects, they are smaller than the observed differences: Grating acuity for 1-month-old infants, for example, is typically 3.5–4.5 octaves lower than that for mature subjects. Therefore we conclude that preneural mechanisms account for many, but not all, of the differences between neonatal and adult contrast sensitivities and grating acuities. The remaining differences must reflect the contribution of postreceptoral mechanisms.

(2) The information loss caused by changes in preneural mechanisms reduces vernier acuity relative to grating acuity. In other words, the difference between vernier and grating acuities, which is a log unit or more in adults, can be substantially reduced by receptoral immaturities in the neonatal fovea. This finding suggests that the differing rates of development for vernier and grating acuities observed in human infants may in part reflect maturation of preneural, rather than cortical, mechanisms.

(3) The failure of young infants to make Rayleigh and neutral-point chromatic discriminations may be caused by poor visual efficiency rather than by immaturities among chromatic mechanisms *per se*. In addition, the improvements in these discriminations observed between the ages of 4 and 12 weeks may reflect improvements in visual efficiency rather than in chromatic mechanisms. On the other hand, the failure of young infants to make tritan discriminations may in fact be a manifestation of a tritan defect.

We have used the term postreceptoral loss to represent the age-related changes that are not explained by our analyses. Our estimates of the magnitude and the character of these losses should be useful in the construction of models of the development of postreceptoral mechanisms.

ACKNOWLEDGMENTS

Several colleagues have generously assisted this project. We thank Bill Geisler for numerous discussions, for developing the ideal observer on which our analyses are based, and for assisting us in installing his Signal Defined Exactly software at Berkeley. We are indebted to Stan Klein, who lent us his work station. We also thank Geoff Owen and Brooke Schefrin for assistance in calculating outer segment efficiencies, Orin Packer and Christine Curcio for providing unpublished data on macaque and human cone dimensions, Tony Adams and Joel Pokorny for helpful discussions about color vision, and Vivianne Smith for pointing out the relevance of the colorimetric purity literature. Finally, we thank Steve Anderson for thorough comments on a preliminary draft, Shalin Kapoor for help in library research, and Davida Teller for excellent editorial assistance. This research was supported by National Institutes of Health research grant HD-19927 (awarded to M. S. Banks).

M. S. Banks is also with the Department of Psychology, University of California, Berkeley.

REFERENCES AND NOTES

1. D. S. Jacobs and C. Blakemore, "Factors limiting the postnatal development of visual acuity in the monkey," Vision Res. **28,** 947–958 (1988).
2. H. R. Wilson, "Development of spatiotemporal mechanisms in infant vision," Vision Res. **28,** 611–628 (1988).
3. G. Bronson, "The postnatal growth of visual capacity," Child Dev. **45,** 873–890 (1974); P. Salapatek, "Pattern perception in early infancy," in *Infant Perception: From Sensation to Cognition*, L. B. Cohen and P. Salapatek, eds. (Academic, New York, 1975), pp. 133–248.
4. A. M. Brown, V. Dobson, and J. Maier, "Visual acuity of human infants at scotopic, mesopic, and photopic luminances," Vision Res. **27,** 1845–1858 (1987).
5. S. Shimojo and R. Held, "Vernier acuity is less than grating acuity in 2- and 3-month-olds," Vision Res. **27,** 77–86 (1987).
6. D. Y. Teller and M. H. Bornstein, "Infant color vision," in *Handbook of Infant Perception*, P. Salapatek and L. B. Cohen, eds. (Academic, New York, 1978), pp. 185–236.
7. W. S. Geisler, "Physical limits of acuity and hyperacuity," J. Opt. Soc. Am. A **1,** 775–782 (1984).
8. W. S. Geisler, "Sequential ideal-observer analysis of visual discriminations," Psychol. Rev. (to be published).
9. D. G. Pelli, "Uncertainty explains many aspects of human contrast detection and discrimination," J. Opt. Soc. Am. A **2,** 1508–1532 (1985); A. B. Watson, H. B. Barlow, and J. G. Robson, "What does the eye see best?" Nature **31,** 419–422 (1983).
10. H. B. Barlow, "Temporal and spatial summation in human vision at different background intensities," J. Physiol. **141,** 337–350 (1958).
11. A. Rose, "The relative sensitivities of television pick-up tubes, photographic film, and the human eye," Proc. IRE **30,** 293–300 (1942).
12. Most of the growth of the eye occurs in the first year. Axial length, for instance, is 16–17 mm at birth, 20–21 mm at 1 year, and 23–25 mm in adolescence and adulthood [see Ref. 13; S. Hirano, Y. Yamamoto, H. Takayama, Y. Sugata, and K. Matsuo, "Ultrasonic observations of eyes in premature babies. Part 6: growth curves of ocular axial length and its components," Acta Soc. Ophthalmol. Jpn. **83,** 1679–1693 (1979)]. Image magnification is proportional to posterior nodal distance [A. G. Bennett and J. L. Francis, "Aberrations of optical images," in *The Eye*, H. Davson, ed. (Academic, New York, 1962)], and so calculations of age-related changes in magnification require estimates of the nodal distance at different ages. The only schematic eyes described for the newborn [J. M. Enoch and R. D. Hamer, "Image size correction of the unilateral aphakic infant," Ophthalmol. Pediatr. Genet. **2,** 153–165 (1983); W. Lotmar, "A theoretical model for the eye of new-born infants," Albrecht von Graefes Archiv. Klin. Exp. Ophthalmol. **198,** 179–185 (1976)] have posterior nodal distances of 10.3–12.0 mm, roughly 2/3 of the adult distance. For a given target in space, then, retinal image size in the eye of the newborn infant should be 2/3 of that in the mature eye. Stated another way, a 1-deg target should subtend 204 μm on the retina of a newborn infant and 298 μm on the retina of an adult.
13. J. S. Larsen, "The sagittal growth of the eye. IV. Ultrasonic measurement of the axial length of the eye from birth to puberty," Acta Ophthalmol. **49,** 873–886 (1971).
14. P. Salapatek and M. S. Banks, "Infant sensory assessment: vision," in *Communicative and Cognitive Abilities: Early Behavioral Assessment*, F. D. Minifie and L. L. Lloyd, eds. (University Park, Baltimore, Md., 1978).
15. S. Stenstrom, "Investigation of the variation and the correlation of the optical elements of human eyes," Am. J. Optom. **25,** 5 (1946).
16. C. Yuodelis and A. Hendrickson, "A qualitative and quantitative analysis of the human fovea during development," Vision Res. **26,** 847–855 (1986).
17. W. H. Miller and G. D. Bernard, "Averaging over the foveal receptor aperture curtails aliasing," Vision Res. **23,** 1365–1370 (1983).
18. We assume a luminance of 50 cd/m^2 for the estimates of pupil diameter. Brown *et al.*[4] also calculated numerical apertures and concluded that the aperture is constant across age under conditions of full dark adaptation and at a luminance of -2.6 log cd/m^2. They argued, however, that the aperture is higher in infants at 0.55 log cd/m^2 and higher. The latter conclusion apparently stems from their own measurements of pupil diameter. This conclusion is inconsistent with that of M. S. Banks, "The development of visual accommodation during early infancy," Child Dev. **51,** 646–666 (1980), who reported that adult pupil diameters are larger than those of 4- to 12-week-old in-

fants at 0.9 log cd/m^2. It is also inconsistent with the data for 1-month-old infants and consistent with the data for 2-month-old infants reported by Salapatek and Banks.[14]

19. R. A. Bone, J. T. Landrum, L. Fernandez, and S. L. Tarsis, "Analysis of macular pigment by HPLC: retinal distribution and age study," Invest. Ophthalmol. Vis. Sci. **29,** 843–849 (1988); J. S. Werner, "Development of scotopic sensitivity and the absorption spectrum of the human ocular media," J. Opt. Soc. Am. **72,** 247–258 (1982). We did not incorporate absorption by retinal structures anterior to the receptors even though the inner nuclear and ganglion cell layers overlay the receptor layer of the central fovea at birth (see Refs. 16 and 20).
20. I. Abramov, J. Gordon, A. Hendrickson, L. Hainline, V. Dobson, and E. LaBossiere, "The retina of the newborn human infant," Science **217,** 265–267 (1982); L. Bach and R. Seefelder, *Atlas zur Entwicklungsgeschichte des Menschlichen Auges* (Englemann, Leipzig, Germany, 1914).
21. Here we give the details of this argument. R. A. Williams and R. G. Boothe ["Development of optical quality in the infant monkey (*Macaca nemestrina*) eye," Invest. Ophthalmol. Vis. Sci. **21,** 728–736 (1981)] measured OTF's in infant and adult *Macaca nemestina*, a species whose visual system at maturity is in many respects similar to the human adult system. Williams and Boothe found that optical transfer is only slightly poorer at birth than in adulthood. They concluded, consequently, that the optical quality of the young macaque eye greatly exceeds the resolution performance of the system as a whole. We do not know whether the optical quality of the human neonate's eye is similar to that of the macaque newborn's eye, but we can estimate the possible contributions of each of several possible optical imperfections: diffraction caused by the pupil, spherical aberration, chromatic aberration, and the clarity of the optic media. Optical degradation as a result of pupillary diffraction should be similar in newborns and adults because their numerical apertures are similar. In regard to spherical and chromatic aberration, unreasonably large amounts would be needed to constrain performance at spatial frequencies of 2 cycles/deg and less. The ocular media could be a significant limit if they were particularly turgid, but ophthalmoloscopic examination reveals clear media in the normal neonate [see, e.g., R. C. Cook and R. E. Glasscock, "Refractive and ocular findings in the newborn," Am. J. Ophthalmol. **34,** 1407–1413 (1951)]. Consequently, pupillary diffraction, spherical and chromatic aberrations, and media clarity probably do not impose significant constraints on early visual performance. Early spatial vision might be constrained by another optical error: inaccurate accommodation. This hypothesis is reasonable because accommodation, like acuity, improves notably during the first months of life.[18] If accommodative error were an important limitation, one would expect the acuity of neonates to vary with target distance. On the contrary, several investigators showed that grating acuity does not vary with distance [See Ref. 22; P. Salapatek, A. G. Bechtold, and E. W. Bushnell, "Infant visual acuity as a function of viewing distance," Child Dev. **47,** 860–863 (1976)]. Thus inaccurate accommodation does not appear to be a significant limitation to neonatal acuity and contrast sensitivity. In sum, the quality of the retinal image almost certainly surpasses the resolution performance of the young visual system. This state of affairs is reminiscent of the retinal periphery in the mature eye.[23] Unlike those in the fovea, peripheral optics are superior to the spatial grain of the receptor lattice. Consequently, adults are able to detect aliasing under conventional viewing conditions [R. A. Smith and P. F. Cass, "Aliasing in the parafovea with incoherent light," J. Opt. Soc. Am. A **4,** 1530–1534 (1987); L. N. Thibos, D. J. Walsh, and F. E. Cheney, "Vision beyond the resolution limit: aliasing in the periphery," Vision Res. **27,** 2193–2197 (1987)]. This raises the intriguing possibility that young infants can detect alias in everyday viewing.
22. J. Atkinson, O. Braddick, and K. Moar, "Development of contrast sensitivity over the first three months of life in the human infant," Vision Res. **17,** 1037–1044 (1977).
23. D. G. Green, "Regional variations in the visual acuity for interference fringes on the retina," J. Physiol. **207,** 351–356 (1970); D. R. Williams, "Aliasing in human foveal vision," Vision Res. **25,** 195–205 (1985).
24. F. W. Campbell and R. W. Gubisch, "Optical quality of the human eye," J. Physiol. **186,** 558–578 (1966).
25. A. Hendrickson and C. Yuodelis, "The morphological development of the human fovea," Ophthalmologica **91,** 603–612 (1984).
26. Our estimates of the diameter of the rod-free zone, the foveola, are based on the data of Ref. 16. The estimate for the adult is slightly larger than that of S. L. Polyak [*The Retina* (U. Chicago Press, Chicago, Ill., 1941)], who reported 1.7–2.0 deg, and much larger than that of G. Oesterberg ["Topography of the layer of rods and cones in the human retina," Acta Ophthalmol. Suppl. **6,** 1–102 (1935)], who reported 1.0 deg. We use the estimate from Ref. 16 because it was obtained with better histological techniques.
27. A completely rigorous treatment would require consideration of physical-optical principles such as diffraction. However, the geometric-optics model is quite accurate when the ratio of stimulus wavelength divided by inner segment diameter is less than 1.0 [R. Winston, "The visual receptor as a light collector," in *Vertebrate Photoreceptor Optics*, J. M. Enoch and F. L. Tobey, Jr., eds. (Springer-Verlag, Berlin, 1981)]. The ratio is less than 0.1 for both central and foveal slope cones in the neonate, so the use of geometric optics is unlikely to distort estimates of the effective collecting areas.
28. There are no quantitative data on the geometry of the newborn cone lattice, but newborn cones are probably roughly triangularly arranged for the following reasons. Inner segment diameters are 64–96% of the cone-to-cone separation in newborns and 74–89% of the cone-to-cone spacing in adults.[16] Thus newborn cones are packed approximately as tightly as are adult cones. Tightly packed lattices tend to adopt triangular (or hexagonal) geometries [A. J. Ahumada and A. Poirson, "Modelling the irregularity of the fovealor mosaic," Invest. Ophthalmol. Vis. Sci. Suppl. **27,** 94 (1986)]. Furthermore, the foveal cone lattice of newborn macques, a species whose retinal development mirrors that of humans, appears more triangular than rectangular [O. Packer, Department of Psychology, University of Washington, Seattle, Washington 98195 (personal communication 1988)]. We assumed for these reasons that the geometry of the newborn lattice is nearly triangular. It does appear, however, that the neonatal foveal cone lattice is somewhat less regular than that of the adult [O. Packer (personal communication, 1988)], but the functional consequences of a slightly irregular lattice are undoubtedly small for most of the tasks considered in this paper. It was shown [W. S. Geisler and K. D. Davila, "Ideal discriminators in spatial vision: two point stimuli," J. Opt. Soc. Am. A **2,** 1483–1492 (1985)], for example, that ideal vernier thresholds are unaffected by moderate changes in lattice regularity. The most-noticeable effects are probably on grating acuity, particularly when performance approaches the Nyquist limit of the receptor lattice [J. I. Yellott, "Consequences of spatially irregular sampling for reconstruction of photon noisy images," Invest. Ophthalmol. Vis. Sci. Suppl. **28,** 137 (1987)].
29. O. Estevez, "On the fundamental data-base of normal and dichromatic color vision," doctoral dissertation (University of Amsterdam, Amsterdam, The Netherlands, 1979).
30. The same ratio was used at all ages for two reasons: (1) The few existing data suggest that all the cones are present before birth [Ref. 16; A. Hendrickson and C. Kupfer, "The histogenesis of the fovea in the macaque monkey," Invest. Ophthalmol. **15,** 746–756 (1976)], so it is unlikely that the proportion of different cone types changes postnatally. It remains possible, however, that one or more cone types are present but dysfunctional early in life, in which case the proportions of functional cones may differ from our assumption. (2) Throughout this paper we have adopted the strategy of assuming that newborn properties are adultlike unless there are data to the contrary.
31. P. L. Walraven, "A closer look at the tritanopic convergence point," Vision Res. **14,** 1339–1343 (1974).
32. M. S. Banks, W. S. Geisler, and P. J. Bennett, "The physical limits of grating visibility," Vision Res. **27,** 1915–1924 (1987).
33. J. Crowell, M. S. Banks, S. J. Anderson, and W. S. Geisler, "Physical limits of grating visibility: fovea and periphery," Invest. Ophthalmol. Vis. Sci. Suppl. **29,** 139 (1988).
34. E. R. Howell and R. F. Hess, "The functional area for summation to threshold for sinusoidal gratings," Vision Res. **18,** 369–

374 (1978); J. J. Koenderink, M. A. Bouman, A. E. Bueno de Mesquita, and S. Slappendel, "Perimetry of contrast detection thresholds of moving spatial sine wave patterns. III. The target extent as a sensitivity controlling parameter," J. Opt. Soc. Am. **68,** 854–860 (1978).

35. For a detailed discussion of the ideal observer that we used, see Refs. 7 and 8. The ideal observer has complete knowledge of the two stimuli to be discriminated and of the Poisson variability associated with them. From this, it constructs a tailored linear weighting function for the specific pair of stimuli. In the case of discriminating a Gabor patch from a uniform field, it constructs a weighting function (a receptive field) that is similar to but not identical to the Gabor patch itself. A stimulus is presented, and if the summed response across the weighted receptor outputs exceeds zero, the observer guesses that the Gabor patch was presented; otherwise it guesses that the uniform field was presented.
36. With small grating patches in a contrast discrimination task,[33] sensitivity of the real observers is within a factor of 4 of ideal contrast sensitivity.
37. A. M. Norcia, Smith-Kettlewell Institute, 2232 Webster Street, San Francisco, California 94115 (personal communication, 1988).
38. F. W. Campbell and J. G. Robson, "Application of Fourier analysis to the visibility of gratings," J. Physiol. **197,** 551–556 (1968).
39. M. S. Banks and P. Salapatek, "Acuity and contrast sensitivity in 1-, 2-, and 3-month-old human infants," Invest. Ophthalmol. **17,** 361–365 (1978); "Infant pattern vision: a new approach based on the contrast sensitivity function," J. Exp. Child Psychol. **31,** 1–45 (1981).
40. M. Pirchio, D. Spinelli, A. Fiorentini, and L. Maffei, "Infant contrast sensitivity evaluated by evoked potentials," Brain Res. **141,** 179–184 (1978); A. M. Norcia, C. W. Tyler, and D. Allen, "Electrophysiological assessment of contrast sensitivity in human infants," Am. J. Optom. Physiol. Opt. **63,** 12–15 (1986).
41. V. Dobson and D. Y. Teller, "Visual acuity in human infants: a review and comparison of behavioral and electrophysiological techniques," Vision Res. **18,** 1469–1483 (1978).
42. A. M. Norcia and C. W. Tyler, "Spatial frequency sweep VEP: visual acuity during the first year of life," Vision Res. **25,** 1399–1408 (1985).
43. We have examined how the parameters chosen for the neonatal ideal observer affect these results. Changes in most of the parameters cause only vertical shifting of the ideal CSF. These include pupil diameter, ocular media transmittance, and outer segment efficiency. Two other parameters cause nearly vertical shifting: receptor aperture and posterior nodal distance. Because ideal contrast sensitivity follows square-root law, an increase in any of these parameters (pupil area, media transmittance, etc.) by itself produces a square-root increase in sensitivity without affecting the shape of the CSF much, if at all. Outer segment efficiency and receptor aperture (which, along with receptor spacing, determines cone coverage) differ most between neonates and adults, so these parameters have by far the largest effects on the relative efficiency of the neonatal ideal observer. Two parameters, the OTF and the assumed spatial summation area, are the primary determinants of the shape of the ideal CSF. In both cases, we assumed adult values.[21,34] Obviously, if optical transfer were significantly worse in neonatal eyes, the high-frequency roll-off of the ideal CSF would be steeper. If summation areas were constant (in degrees) across spatial frequency, the high-frequency roll-off would be shallower.
44. Two pieces of evidence suggest, but by no means prove, that newborns fixate visual targets foveally: (1) Neonates seem to use a consistent retinal locus when fixating a high-contrast target [Ref. 3; L. Hainline and C. Harris, "Does foveal development influence the consistency of infants' point of visual regard?" Infant Behav. Dev. **11,** 129 (1988); A. M. Slater and J. M. Findlay, "Binocular fixation in the newborn baby," J. Exp. Child Psychol. **20,** 248–273 (1975)]. It was not demonstrated, however, that this locus is the fovea because of uncertainties about the location of the visual axis with respect to the optic axis. (2) Retinal and central nervous development in macaques and humans is similar, except that macaques are somewhat more advanced at birth and mature more rapidly [R. G. Boothe, R. A. Williams, L. Kiorpes, and D. Y. Teller, "Development of contrast sensitivity in infant *Macaca nemestrina* monkeys," Science **208,** 1290–1292 (1980); P. M. Kiely, S. G. Crewther, J. Nathan, N. A. Brennan, N. Efron, and M. Madigan, "A comparison of ocular development of the cynomolgus monkey and man," Clin. Vis. Sci. **3,** 269–280 (1987); Ref. 30]. C. Blakemore and F. Vital-Durand ["Development of the neural basis of visual acuity in monkeys. Speculation on the origin of deprivation amblyopia," Trans. Ophthalmol. Soc. U.K. **99,** 363–368 (1980)] measured the visual resolution of lateral geniculate nucleus cells supplied by different retinal regions. They found much higher resolution among cells supplied by the fovea than among cells supplied by the periphery in 21-week-old and adult macaques. In newborn macaques, the acuity of foveal cells was diminished but still higher than the acuity of peripheral cells. Thus, in macaque infants anyway, the highest resolution is likely to be observed with central vision. The same appears to be true for human infants. T. L. Lewis, D. Maurer, and D. Kay ["Newborns' central vision: whole or hole?" J. Exp. Child Psychol. **26,** 193–203 (1978)] found that newborns could detect a narrower light bar against a dark background when it was presented in central vision than when it was presented in the periphery. These pieces of evidence suggest that newborn contrast sensitivity and acuity estimates are manifestations of central rather than peripheral processing, but more direct experimental evidence clearly is needed to settle the issue.
45. D. M. Levi and S. A. Klein, "Hyperacuity and amblyopia," Nature **298,** 268–270 (1982).
46. D. M. Levi, S. A. Klein, and A. P. Aitsebaomo, "Vernier acuity, crowding, and cortical magnification," Vision Res. **25,** 963–977 (1985).
47. G. Westheimer, "The spatial grain of the perifoveal visual field," Vision Res. **22,** 157–162 (1982).
48. R. E. Manny and S. A. Klein, "The development of vernier acuity in infants," Curr. Eye Res. **3,** 453–462 (1984).
49. R. E. Manny and S. A. Klein, "A three-alternative tracking paradigm to measure vernier acuity of older infants," Vision Res. **25,** 1245–1252 (1985).
50. S. Shimojo, E. E. Birch, J. Gwiazda, and R. Held, "Development of vernier acuity in infants," Vision Res. **24,** 721–728 (1984).
51. D. Allen, P. J. Bennett, and M. S. Banks, "Effects of luminance on FPL and VEP acuity in human infants," Invest. Ophthalmol. Vis. Sci. Suppl. **28,** 5 (1987); V. Dobson, D. Salem, and J. B. Carson, "Visual acuity in infants—the effect of variations in stimulus luminance within the photopic range," Invest. Ophthalmol. Vis. Sci. **24,** 519–522 (1983).
52. D. R. Peeples and D. Y. Teller, "Color vision and brightness discrimination in two-month-old infants," Science **189,** 1102–1103 (1975).
53. D. Y. Teller, D. R. Peeples, and M. Sekel, "Discrimination of chromatic from white light by two-month-old human infants," Vision Res. **18,** 41–48 (1978).
54. R. D. Hamer, K. Alexander, and D. Y. Teller, "Rayleigh discriminations in young human infants," Vision Res. **22,** 575–588 (1984).
55. O. Packer, E. E. Hartmann, and D. Y. Teller, "Infant color vision: the effect of test field size on Rayleigh discriminations," Vision Res. **24,** 1247–1260 (1984).
56. D. Varner, J. E. Cook, M. E. Schneck, M. A. McDonald, and D. Y. Teller, "Tritan discrimination by 1- and 2-month-old human infants," Vision Res. **25,** 821–831 (1985).
57. In retrospect, the data are not really consistent with this hypothesis because the failure to discriminate yellow-greens from yellowish-white is, if anything, more consistent with a protan or deutan defect.
58. There are two methodological shortcomings in the studies of R. J. Adams, D. Maurer, and M. Davis ["Newborns' discrimination of chromatic from achromatic stimuli," J. Exp. Child Psychol. **41,** 267–281 (1986)] and D. Maurer and R. J. Adams ["Emergence of the ability to discriminate a blue from gray at one month of age," J. Exp. Child Psychol. **44,** 147–156 (1987)]. First and most important, they did not vary the intensity of their chromatic stimuli for each infant. Instead, different intensities

were presented to different groups of children. If group looking times were, at all intensities, significantly greater to the chromatic checkerboards than to the uniform fields, they concluded that infants were able to differentiate on the basis of hue alone. If dips in performance were observed at particular check intensities, they concluded that infants based their responses on brightness cues. The validity of the former conclusion hinges on the untested assumption that equiluminant points are similar for all infants of a given age. If such points vary from child to child, the absence of performance dips does not rule out the possibility that some infants based their looking preferences on brightness at each stimulus intensity. Second, even if equiluminance did not vary significantly across children, the performance criterion of Maurer and Adams was much more lenient than that of Teller. Maurer and Adams required only that looking times be statistically significantly greater with the checkerboards than with the uniform field. Teller and colleagues[52–56] required at least 70% correct performance from each infant at all stimulus intensities.

59. K. T. Mullen, "The contrast sensitivity of human color vision to red/green and blue/yellow chromatic gratings," J. Physiol. **359,** 381–400 (1985).
60. E. M. Granger and J. C. Heurtley, "Visual chromaticity modulation transfer function," J. Opt. Soc. Am. **63,** 1173–1174 (1973); D. H. Kelly, "Spatiotemporal variation of chromatic and achromatic contrast thresholds," J. Opt. Soc. Am. **73,** 742–750 (1983); G. J. C. van der Horst, C. M. M. de Weert, and M. A. Bouman, "Transfer of spatial chromaticity-contrast at threshold in the human eye," J. Opt. Soc. Am. **57,** 1260–1266 (1967).
61. C. F. Stromeyer III, G. R. Cole, and R. E. Kronauer, "Second-site adaptation in the red-green chromatic pathways," Vision Res. **25,** 219–238 (1985).
62. The ideal observer of Table 1 follows square-root law in chromatic contrast sensitivity tasks. G. J. C. van der Horst and M. A. Bouman ["Spatio-temporal chromaticity discrimination," J. Opt. Soc. Am. **59,** 1482–1488 (1969)] measured contrast sensitivity with isoluminant gratings for a wide range of photopic illuminances. They found that chromatic contrast sensitivity (defined in a fashion similar to that in Ref. 59) increased as the square-root of illuminance from 1.2 to 160 photopic trolands, the highest light level presented. Square-root law only held for frequencies greater than 3 cycles/deg; at lower frequencies, Weber's law was observed at the higher illuminances. Thus, as with luminance contrast sensitivity,[32,33] the luminance dependence of ideal chromatic contrast sensitivity is similar to that of real observers, at least for intermediate to high spatial frequencies.
63. A. M. Derrington, J. Krauskopf, and P. Lennie, "Chromatic mechanisms in lateral geniculate nucleus of macaque," J. Physiol. **357,** 241–265 (1984); R. L. De Valois, I. Abramov, and G. H. Jacobs, "Analysis of response patterns of LGN cells," J. Opt. Soc. Am. **56,** 966–977 (1966).
64. To understand this, it is useful to consider an isoluminant red–green grating separated into its two components: a red–black grating and a green–black grating. When the red component is presented, LWS cones respond in rough proportion to the luminance variation from the peak to the trough of the grating. They also respond in this way, though at somewhat reduced levels, to the green component. When the red and green grating components are added in phase, producing a yellow–black grating, the LWS cone modulations that are due to each component add, producing a large overall modulation. When the components are added in opposite phase, producing an isoluminant red–green grating, the LWS cone modulations to each component cancel to some degree, and the overall modulation is smaller. The same reasoning obviously applies to the MWS cones.
65. There is indirect evidence that all three cone types are functional at birth. D. R. Peeples and D. Y. Teller ["White-adapted photopic spectral sensitivity in human infants," Vision Res. **18,** 49–53 (1978)] and A. Moskowitz-Cook ["The development of photopic spectral sensitivity in human infants," Vision Res. **18,** 1133–1142 (1979)] showed that the photopic spectral sensitivity of infants is similar to that of adults. Their observations suggest that MWS and LWS cones are functional early in life. The small differences between neonatal and adult photopic spectral sensitivities probably are explained by age-related changes in the ocular media.[19] V. J. Volbrecht and J. S. Werner ["Isolation of short-wavelength-sensitive cone photoreceptors in 4–6-week-old human infants," Vision Res. **27,** 469–478 (1987)] used a chromatic adaptation paradigm to demonstrate the presence of SWS cones in young infants. Although the results of these three studies imply the existence of three functional cone types, they do not indicate whether the infant visual system can preserve and compare signals from one cone type to another. Moreover, the data of Volbrecht and Werner do not inform us about the relative sensitivity of SWS cones early in life.
66. Because neonatal outer segments are shorter than adult segments, they probably exhibit less self-screening.[67] In consequence, neonatal action spectra should be narrower than adult spectra. We have not incorporated this effect into the newborn ideal observer because it is likely to be quite small for the tasks that we consider. It should be noted, however, that the narrowing of action spectra should cause the color-matching and luminosity functions of neonates to differ from those of adults. For instance, one would predict that the green–red setting in an anomaloscopelike experiment would be lower in infants' central vision just as it is in adults' peripheral vision [J. Pokorny and V. C. Smith, "Effect of field size on red–green color mixture equations," J. Opt. Soc. Am. **66,** 705–708 (1976)]. In addition, one would predict the relative luminous efficiency of long-wavelength lights to be lower in neonates' central vision. Interestingly, Hamer *et al.*,[54] Packer *et al.*,[55] and J. E. Clavadetscher ["Young infants show a relative insensitivity to long wavelength (red) light," Infant Behav. Dev. Suppl. **11,** (1988)] reported such an effect in young infants.
67. G. Wyszecki and W. S. Stiles, *Color Science: Concepts and Methods, Quantitative Data, and Formulae* (Wiley, New York, 1982).
68. For details on the ideal observer's decision strategy in such tasks, consult Ref. 8. When asked to discriminate a 550-nm target in a 589-nm background from a uniform 589-nm background, the ideal observer constructs a weighting function consisting of positive weights for MWS cone stimulation in the target region and negative weights for LWS cone stimulation in the same region. When the summed response exceeds zero, the ideal observer guesses that the 550-nm target was presented.
69. Increment and decrement thresholds of real infants are nearly identical when expressed in log units.[53]
70. Some of the parameters of the neonatal ideal observer affect the predictions of the visual efficiency hypothesis and some do not. Pupil diameter, posterior nodal distance, receptor aperture, receptor spacing, the optical transfer function, and spatial summation area do not affect predictions at all because luminance and chromatic thresholds are affected similarly by changes in these parameters. Three parameters do influence predictions: (1) Ocular media transmittance: we assumed a higher transmittance for neonates.[19] The media are nearly transparent at long wavelengths, so predictions for the Rayleigh[54,55] and neutral-point[52,53] experiments are virtually unaffected by the range of transmittances that we used. Predictions for the tritan experiment,[56] however, are in fact affected by the media: the lighter the media, the lower the chromatic threshold of the neonatal ideal observer. (2) Relative numbers of the three cone types: within reasonable variations of the relative proportions of cone types, predictions do not vary significantly. (3) Outer segment length: self-screening affects the bandwidth of receptor absorption spectra.[67] In long outer segments, self-screening is more pronounced and absorption spectra broaden. Thus neonatal foveal cones may well have narrower spectra than we assumed. The consequence of narrower spectra is an improvement in many chromatic discriminations relative to luminance discriminations. The effect is not large, however, for the chromatic tasks that we examined, so we do not incorporate it here.
71. I. G. Priest and F. G. Brickwedde, "The perceptible colorimetric purity as a function of dominant wavelength," J. Opt. Soc. Am. **28,** 133–139 (1938); W. D. Wright, *Researches on Normal and Defective Colour Vision* (Klimpton, London, 1946).
72. V. C. Smith, R. W. Bowen, and J. Pokorny, "Threshold temporal integration of chromatic stimuli," Vision Res. **24,** 653–660 (1984).

73. H. R. Wilson and D. J. Gelb, "Modified line element theory for spatial frequency and width discrimination," J. Opt. Soc. Am. A **1,** 124–131 (1984).
74. D. I. A. MacLeod, "Visual sensitivity," Annu. Rev. Psychol. **29,** 613–645 (1978).
75. D. C. Hood, "Sensitivity to light," in *Handbook of Perception and Human Performance*, K. R. Boff, L. Kaufman, and J. P. Thomas, eds. (Wiley, New York, 1986), pp. 5-1–5-66. The equation that we used to calculate half-bleaching constants is

$$(1 - p)/T_0 = I[1 - \exp(-Dp)]/(DQ_e),$$

where p is the proportion of unbleached pigment, T_0 is the regeneration time constant, I is the steady retinal illuminance in trolands, D is the optical density, and Q_e is the photosensitivity of the receptor in troland-seconds. The half-bleaching constants reported in the text should be modified slightly to reflect the differences in effective apertures of newborn and adult cones. If we make the assumption that 80% of the quanta incident upon the adult inner segment are transmitted to the outer segment, the adult half-bleaching illuminance is reduced by 0.3 log unit relative to the newborn value.
76. M. S. Banks and J. L. Dannemiller, "Infant visual psychophysics," in *Handbook of Infant Perception*, P. Salapatek and L. B. Cohen, eds. (Academic, New York, 1987), pp. 115–184.
77. R. D. Hamer and M. E. Schneck, "Spatial summation in dark-adapted human infants," Vision Res. **24,** 77–85 (1984); A. B. Fulton, R. M. Hansen, and C. W. Tyler, "Temporal summation in human infants," Invest. Ophthalmol. Vis. Sci. Suppl. **29,** 60 (1988).
78. J. Atkinson and O. J. Braddick, "Development of optokinetic nystagmus in infants: an indicator of cortical binocularity?" in *Eye Movements: Cognition and Visual Perception*, D. F. Fisher, R. A. Monty, and J. W. Senders, eds. (Erlbaum, Hillsdale, N.J., 1981), pp. 53–64; M. S. Banks, B. R. Stephens, and E. E. Hartmann, "The development of basic mechanisms of pattern vision: spatial frequency channels," J. Exp. Child Psychol. **40,** 501–527 (1985); O. Braddick and J. Atkinson, "Sensory selectivity, attentional control, and cross-channel integration in early visual development," in *Perceptual Development in Infancy: The Minnesota Symposium on Child Psychology*, A. Yonas, ed. (Erlbaum, Hillsdale, N.J., 1987), pp. 105–143; O. Braddick, J. Wattam-Bell, and J. Atkinson, "Orientation-specific cortical responses develop in early infancy," Nature **320,** 617–619 (1986).
79. A. B. Bonds, "Development of orientation tuning in the visual cortex of kittens," in *Developmental Neurobiology of Vision*, R. D. Freeman, ed. (Plenum, New York, 1979); A. M. Derrington and A. F. Fuchs, "The development of spatial-frequency selectivity in kitten striate cortex," J. Physiol. **316,** 1–10 (1981); D. H. Hubel and T. N. Wiesel, "Receptive fields of cells in striate cortex of very young, visually inexperienced kittens," J. Neurophysiol. **26,** 994–1002 (1963).
80. D. I. Hamasaki and J. T. Flynn, "Physiological properties of retinal ganglion cells of 3-week-old kittens," Vision Res. **17,** 275–284 (1977).
81. This idea was suggested by W. S. Geisler, Department of Psychology, University of Texas, Austin, Texas 78712 (personal communication, 1988).
82. C. Blakemore and F. W. Campbell, "On the existence of neurons in the human visual system selectively sensitive to the orientation and size of retinal images," J. Physiol. **203,** 237–260 (1969); F. W. Campbell and J. J. Kulikowski, "Orientational selectivity of the human visual system," J. Physiol. **187,** 437–445 (1966).
83. J. L. Dannemiller and M. S. Banks, "The development of light adaptation in human infants," Vision Res. **23,** 599–609 (1983); R. M. Hansen and A. B. Fulton, "Behavioral measurement of background adaptation in infants," Invest. Ophthalmol. Vis. Sci. **21,** 625–629 (1981).
84. D. H. Kelly, "Visual contrast sensitivity," Opt. Acta **24,** 107–129 (1977).
85. J. A. Movshon and L. Kiorpes, "Analysis of the development of spatial contrast sensitivity in monkey and human infants," J. Opt. Soc. Am. A **5,** 2166–2172 (1988).
86. A. Watson, "The ideal observer concept as a modeling tool," in *Frontiers of Visual Science: Proceedings of the 1985 Symposium* (National Academy of Sciences, Washington, D.C., 1987), pp. 32–37.